J/ψ plus W or Z Production: Consequences for NLO LDME Fits

Mathias Butenschön
(Universität Hamburg)

1. Introduction to NRQCD Factorization
2. New Results for pp $\longrightarrow$ J/ψ + W or Z
3. NLO Fits of NRQCD: State After new Results

1.1 Production of Quarkonium

- **Heavy Quarkonia:** Bound states of heavy quark and antiquark.
- The classic approach: **Color Singlet Model**
  - Calculate cross section for heavy quark pair in physical **color singlet** (=color neutral) state. In case of J/ψ: $c\bar{c}[\,^3S_1^{[1]}]$
  - Multiply by quarkonium wave function at origin
  - Leftover IR singularities in case of *P* wave quarkonia
  - Mid 90's: Strong disagreement with Tevatron data apparent
- **Nonrelativistic QCD (NRQCD):**
  - Rigorous effective field theory [Bodwin, Braaten, Lepage (1995)]
  - Based on **factorization of soft and hard scales** (Scale hierarchy: $Mv^2 \ll Mv \approx \Lambda_{QCD} \ll M$)
- Other prominent model: Color Evaporation Model
- Open Question: **Is NRQCD factorization compatible with data?**

1.2 Quarkonium Production with NRQCD

- **Factorization theorem:** $\sigma_H = \sum_n \sigma_{Q\bar{Q}[n]} \cdot \langle O^H[n] \rangle$
  - n: Every possible Fock state, including color-octet (CO) states
  - $\sigma_{Q\bar{Q}[n]}$: Production rate of $Q\bar{Q}[n]$, calculated in perturbative QCD
  - $\langle O^H[n] \rangle$: Nonperturbative long distance matrix elements (**LDMEs**): Describe $Q\bar{Q}[n] \to H$, supposedly universal, taken from fits to data
- **Scaling rules** (here $H = J/\psi$):

Scaling	v^3	v^7 ("CO states")	v^{11}
n	${}^3S_1^{[1]}$	${}^1S_0^{[8]}$, ${}^3S_1^{[8]}$, ${}^3P_J^{[8]}$	…

  - Double expansion in α_s und v
  - Leading term in v expansion (${}^3S_1^{[1]}$) equals Color-Singlet Model
- Key test for NRQCD factorization: **Are the LDMEs universal?**
  ⟹ Fit LDMEs to some observables and predict other observables.

1.3 The NRQCD Calculations

- **Factorization formulas** (here J/ψ hadroproduction):

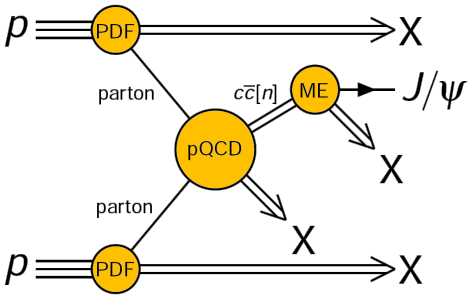

- **Convolute partonic cross section with PDFs:**

$$\sigma_{\text{hadr}} = \sum_{i,j} \int dx\, dy\, f_{i/p}(x)\, f_{j/p}(y) \cdot \sigma_{\text{part,i,j}}$$

- **NRQCD factorization:**

$$\sigma_{\text{part,i,j}} = \sum_{n} \sigma(ij \to c\bar{c}[n] + X) \cdot \langle O^{J/\psi}[n] \rangle$$

- Amplitudes for $Q\bar{Q}[n]$ production by **projector** application, e.g.

$$A_{Q\bar{Q}[^3S_1^{[1/8]}]} = \varepsilon_\alpha \,\mathrm{Tr}\left[C\,\Pi^\alpha A_{Q\bar{Q}}\right]|_{q=0}$$

$$A_{Q\bar{Q}[^3P_J^{[1/8]}]} = \varepsilon_{\alpha\beta}\,\frac{d}{dq_\beta}\,\mathrm{Tr}\left[C\,\Pi^\alpha A_{Q\bar{Q}}\right]|_{q=0}$$

Derivatives ⟹ Larger expressions, higher propagator powers, non-standard IR singularity structure.

- $A_{Q\bar{Q}}$: Amputated pQCD amplitude for open $Q\bar{Q}$ production
- q: Relative momentum between Q and $\bar{Q}$
- ϵ: Quarkonium polarization vectors

2.1 $pp \longrightarrow J/\psi$ + W or Z

- **Experimental data:**
  - $pp \longrightarrow J/\psi + W^{\pm} + X$ [ATLAS (2014); ATLAS (2020)]
  - $pp \longrightarrow J/\psi + Z + X$ [ATLAS (2015)]
- **Born** calculations: [Kniehl, Palisoc, Zwirner (2002)]
  - Additional contrib. in $c\bar{c}[\,^3S_1^{[1]}] + W^{\pm}$ [Lansberg, Lorcé (2013)]
- Previous **NLO** calculations:
  - $pp \longrightarrow c\bar{c}[\,^1S_0^{[8]}, {}^3S_1^{[8]}, {}^3P_J^{[8]}] + W^{\pm} + X$ [Li, Song, Zhang, Ma (2011)]
  - $pp \longrightarrow c\bar{c}[\,^3S_1^{[1]}, {}^3S_1^{[8]}] + Z + X$ [Song, Ma, Li, Zhang, Guo (2011)]
  - $pp \longrightarrow c\bar{c}[\,^3S_1^{[1]}] + Z + X$ (+polarization) [Gong, Lansberg, Lorcé, Wang (2013)]
- **This Work:** Analysis with missing channels (also $\psi(2S)$ and χ_{cJ} feeddown)
  - $pp \longrightarrow c\bar{c}[\,^1S_0^{[8]}, {}^3P_J^{[8]}, {}^3P_J^{[1]}] + Z + X$ at NLO
  - $pp \longrightarrow c\bar{c}[\,^3P_J^{[1]}] + W^{\pm} + X$ at NLO
- **Most complex** NLO NRQCD calculation so far, because ***P* state virtual corrections** and **additional *W/Z* mass scale.**

2.2 Contributions and Example Diagrams

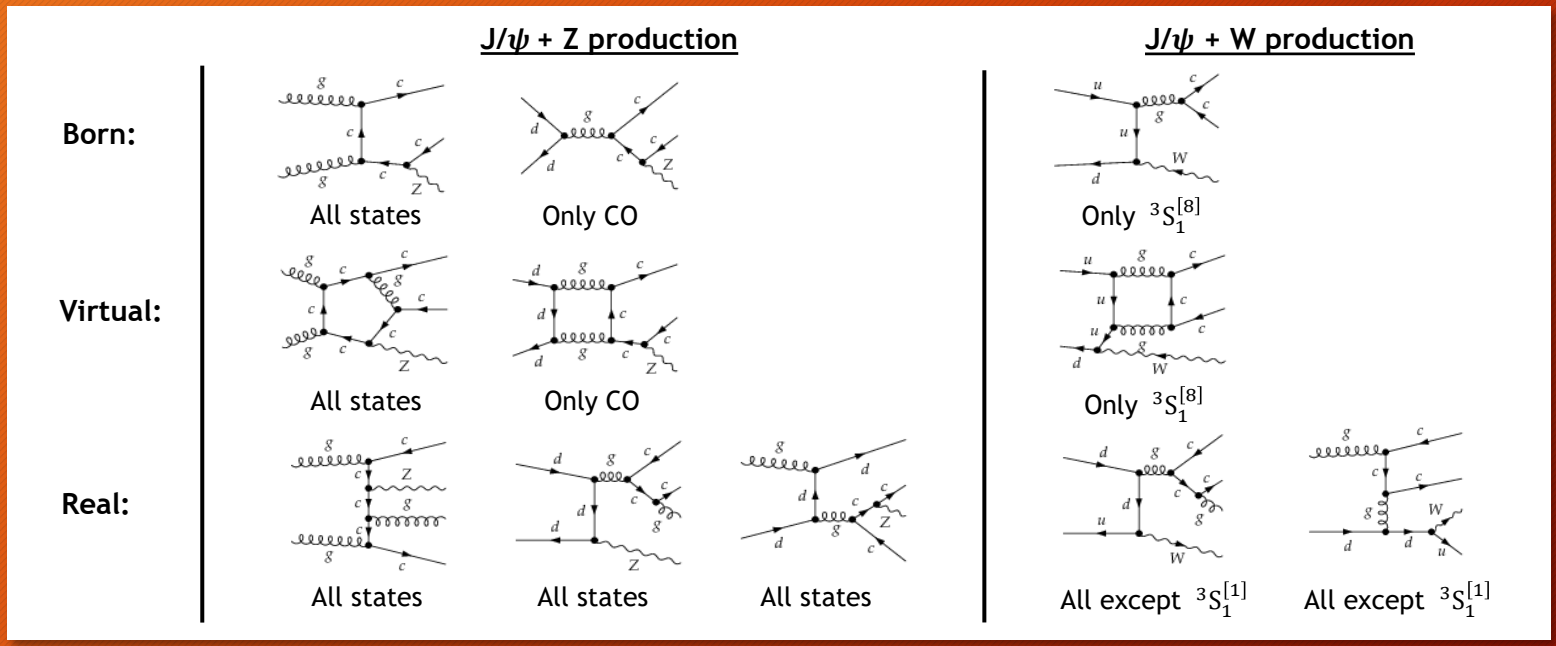

- $J/\psi + W^{\pm}$: At LO only $^3S_1^{[8]}$, and $^3S_1^{[1]}$ not even at NLO:
  - **Much simpler** to calculate than $J/\psi + Z$ (No *P* state virtual corrections)
  - Caution: Formally NLO, but actually LO?
    For $^3S_1^{[1]}$ not even leading contributions considered.

2.3 Organization of the NLO Calculation

Diagram generation with FeynArts

FORM and Mathematica: Treat squared amplitudes

Two Methods for Virtual Corrections:

FORM: Our generalization of Passarino-Veltman reduction ⟶ Scalar integrals

FORM/AIR: IBP ⟶ Master integrals

FORM/AIR: Cancel scalar products by denominators and directly apply IBP

Mathematica script: Simplification (few GB ⟶ few MB)

Two Methods for Cross Section Evaluation:

Phase space slicing implementation

Dipole subtraction building on Catani/Seymour and Phaf/Weinzierl

- *New:* Structure of singularities for bound states
- *New:* Additional dipoles for P states

[MB, Kniehl: NPB 905 (2020) 114843, NPB 957 (2020) 115056]

2.4 Scale Choices

- **Renormalization** and **factorization** scale μ_r and μ_f choices:
  1. $\mu_r = \mu_f = m_{T,J/\psi}$ [Song, Ma, Li, Zhang, Guo (2011)]
  2. $\mu_r = \mu_f = \sqrt{m_{T,J/\psi} m_{T,W/Z}}$ [Kniehl, Palisoc, Zwirner (2002)]
  3. $\mu_r = \mu_f = M_{W/Z}$ [Gong, Lansberg, Lorcé, Wang (2013)]

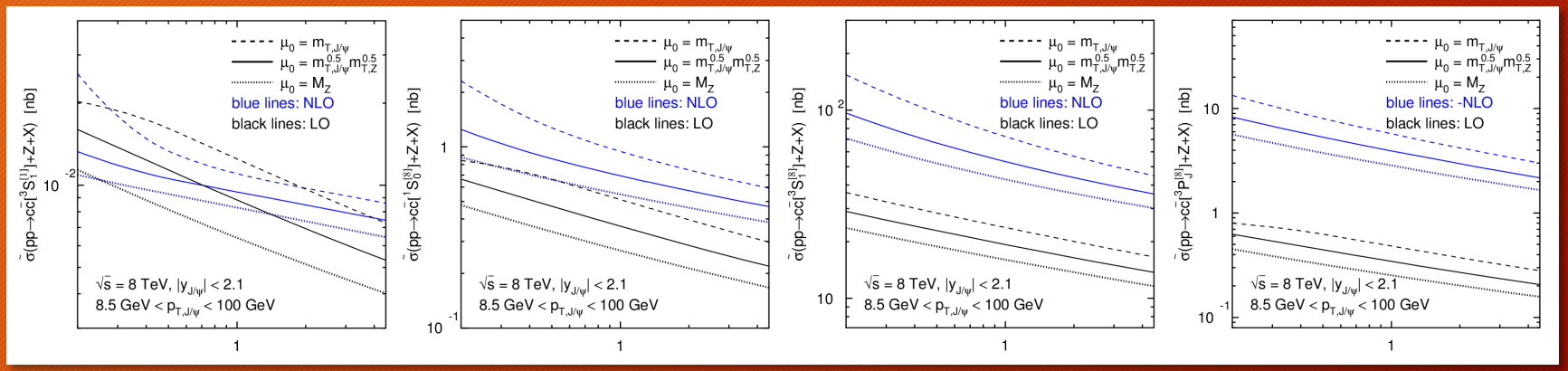

- $M_{W/Z}$ and $\sqrt{m_{T,J/\psi} m_{T,W/Z}}$: Smaller NLO scale dependence compared to $m_{T,J/\psi}$.
- $m_{T,J/\psi}$ and $\sqrt{m_{T,J/\psi} m_{T,W/Z}}$: Particularly small *K* factor in $c\bar{c}[\,^3S_1^{[1]}] + Z$.

⇨ Use $\mu_r = \mu_f = \sqrt{m_{T,J/\psi} m_{T,W/Z}}$, but **vary scales by factor 4** up and down.

2.5 Double Parton Scattering

- We calculate single parton scattering (SPS).
  But J/ψ and W/Z may originate from **different partonic interactions**
  $\Longrightarrow$ **Double parton scattering** (DPS)
- Usual DPS model: The two partonic interactions are independent, double parton PDFs factorize into single parton PDFs.

  $\Longrightarrow$ **Pocket formula:** $\sigma_{DPS} = \frac{\sigma_{J/\psi}\sigma_{W/Z}}{\sigma_{\mathrm{eff}}}$ with σ_{eff} universal „effective scattering area“
- In ATLAS J/ψ + W or Z papers: DPS contributions estimated using $\sigma_{\mathrm{eff}} = 15^{+5,8}_{-4,2}$ mb from ATLAS W + 2 jet measurement:

Table 5 The inclusive (SPS + DPS) cross-section ratio $dR^{\mathrm{incl}}_{Z+J/\psi}/dp_T$ for prompt and non-prompt J/ψ. Estimated DPS contributions for each bin, based on the assumptions made in this study, are presented

$p_T^{J/\psi}$ (GeV)	Inclusive prompt ratio ($\times 10^{-7}$/GeV) value ± (stat) ± (syst) ± (spin)			Estimated DPS ($\times 10^{-7}$/GeV) assuming $\sigma_{\mathrm{eff}} = 15$ mb
(8.5, 10)	10.8 ± 5.6	±1.9	±3.1	5.5 ± 2.1
(10, 14)	5.6 ± 1.9	±0.8	±1.2	1.7 ± 0.6
(14, 18)	1.9 ± 1.1	±0.1	±0.3	0.4 ± 0.1
(18, 30)	0.87 ± 0.37	±0.12	±0.09	0.05 ± 0.02
(30, 100)	0.090 ± 0.037	±0.012	±0.006	0.0004 ± 0.0002

- We compare to **DPS subtracted data.**
- **Minor role of DPS** supported by measurement of **angular distribution $\Delta\phi$**
  (SPS: Peak at back-to-back,
  DPS: Random distribution)

2.6 Results for J/ψ + Z

- Predictions using different LDME sets. **Uncertainty bands** due to
  1. Renormalization and factorization scale variation: $\frac{1}{4} < \mu_r = \mu_f < 4$
  2. NRQCD scale variation: $\frac{1}{2} < \mu_\Lambda < 2$
  3. LDME fit errors (assuming no correlations)

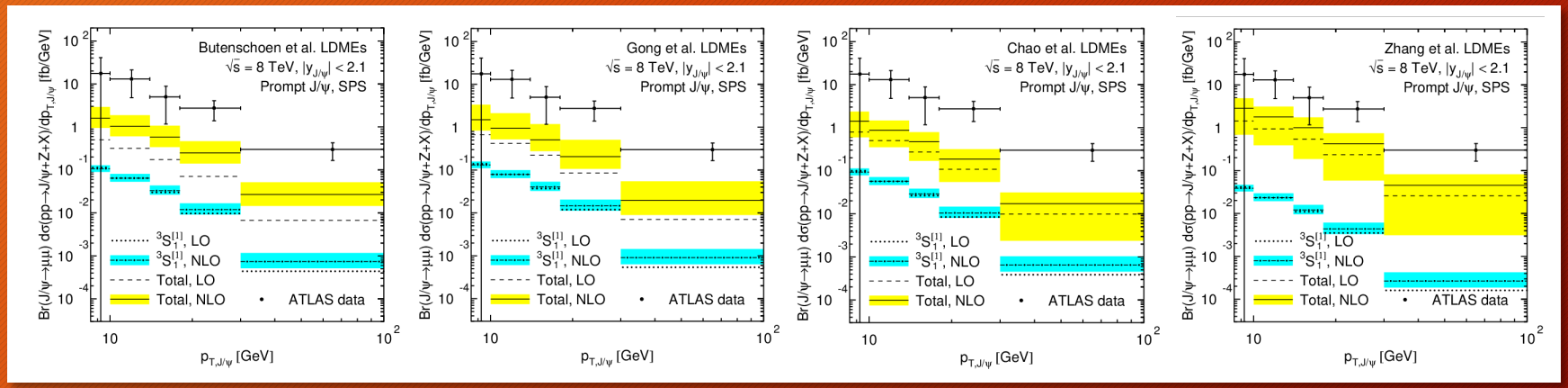

- $^3S_1^{[1]}$: LO $\longrightarrow$ NLO stable. Including CO: **Reasonable *K* factors** (<6). CO important.
- Predictions **factor 10 below data.** If difference due to DPS, DPS would need to be 10 times larger than SPS, contradicting physics picture and $\Delta\phi$ measurement.

2.7 Results for J/ψ + $W^{\pm}$

- **Similar picture** for J/ψ + W production
  (Reminder: We have no $^3S_1^{[1]}$ contributions here.)

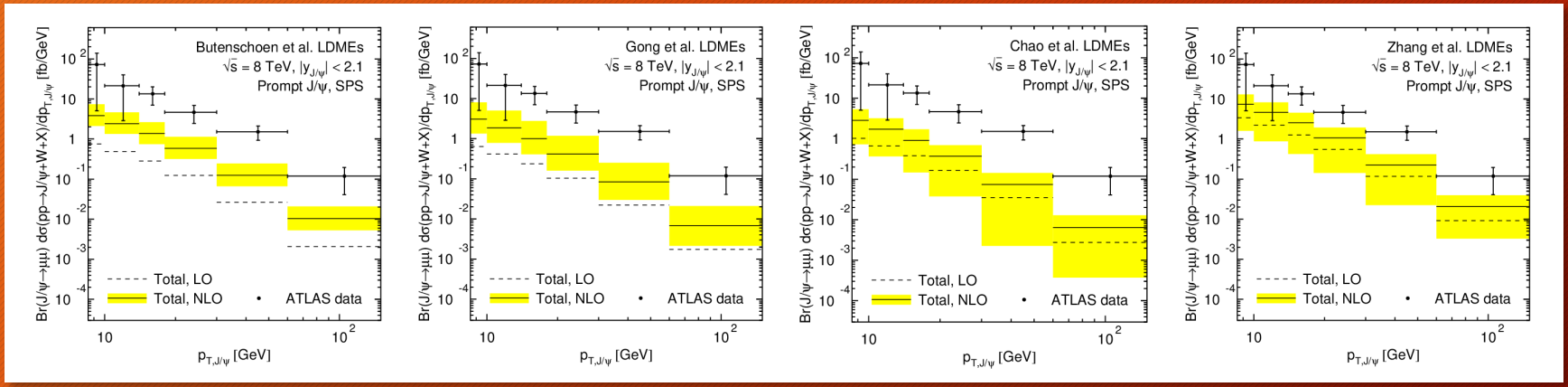

- NRQCD predictions for all LDME sets **fall short of data** by factor 10.
- Caution: For all states except $^3S_1^{[8]}$, NLO is actually leading order.
  ⇨ **Large NNLO** corrections can be expected.

3.1 NLO LDME Fits

- **CS LDME $\langle O^{J/\psi}(^3S_1^{[1]})\rangle$:** Usually not fitted, but from $\Gamma(J/\psi \longrightarrow e^+e^-)$ or potential model
- **Fitted CO LDMEs:** $\langle O^{J/\psi}(^1S_0^{[8]})\rangle$, $\langle O^{J/\psi}(^3S_1^{[8]})\rangle$, $\langle O^{J/\psi}(^3P_0^{[8]})\rangle$
- Some fits consider **$\psi(2S)$, χ_{cJ} feeddown:**
  - Corresponding CS LDMEs again usually from decay rates/potential models.
  - Fit CO LDMEs $\langle O^{J/\psi}(^1S_0^{[8]})\rangle$, $\langle O^{J/\psi}(^3S_1^{[8]})\rangle$, $\langle O^{J/\psi}(^3P_0^{[8]})\rangle$; $\langle O^{\chi_{c0}}(^3S_1^{[8]})\rangle$.
- **Data fitted to:**
  - J/ψ hadroproduction with transverse momentum $p_T > 7$ GeV included in all fits.
  - Different fits include different further observables.
- In the following:
  - Take LDME sets **from 6 fits** and give predictions for: J/ψ photoproduction, hadroproduction of J/ψ (+polarization), η_c and $J/\psi + Z$. (Selection criteria: Full NLO calculations and sufficiently precise data available)
  - **η_c (h_c) LDMEs** are related to J/ψ (χ_{c0}) LDMEs via **heavy quark spin symmetry.**
  - Uncertainty bands: Only **scale variations** everywhere

3.2 Butenschön et al. LDMEs

J/ψ Photoproduction

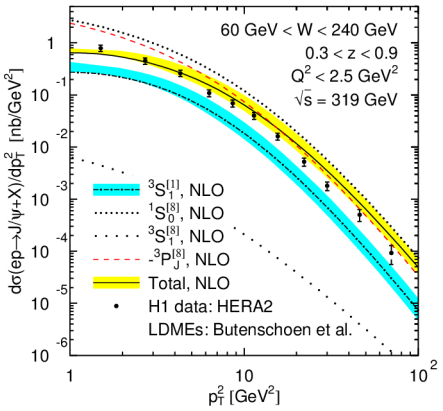

J/ψ Hadroproduction

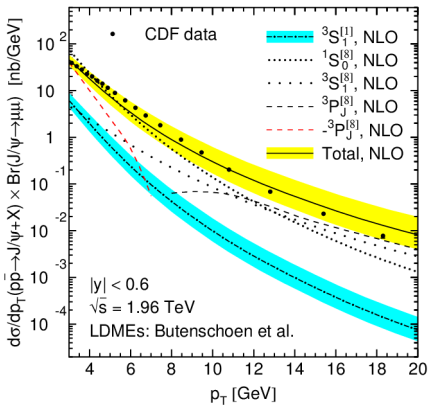

η_c Hadroproduction

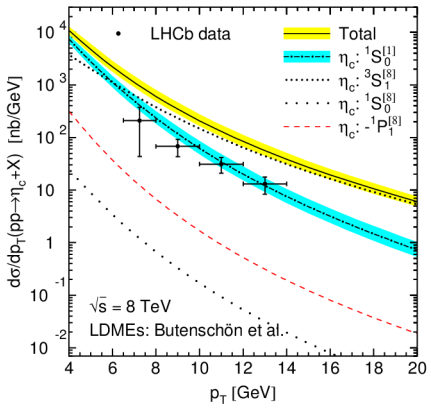

J/ψ + Z Hadroproduction

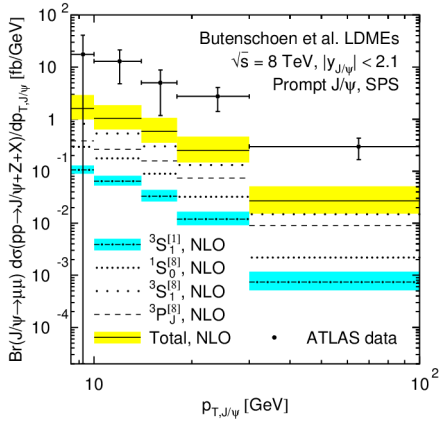

J/ψ Polarization (CDF)

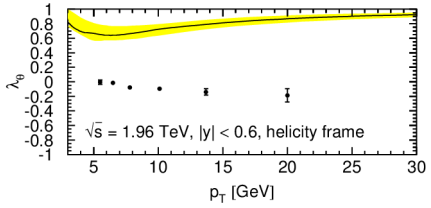

J/ψ Polarization (LHCb)

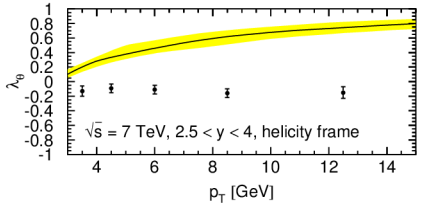

- Fit to 194 data points of J/ψ photo- and hadro-production, $\gamma\gamma$- and e^+e^- scattering
- $\langle O^{J/\psi}(1S08)\rangle = 4.97 \pm 0.44$, $\langle O^{J/\psi}(3S18)\rangle = 0.22 \pm 0.06$, $\langle O^{J/\psi}(3P08)\rangle = -1.61 \pm 0.20$ [in 10^{-2} GeV^3 or 10^{-2} GeV^5]
- Ref.: [MB, Kniehl, PRD 84, 051501 (2011)]

- Data fitted to is described within scale uncertainties, other observables not.

3.3 Gong et al. LDMEs

J/ψ Photoproduction

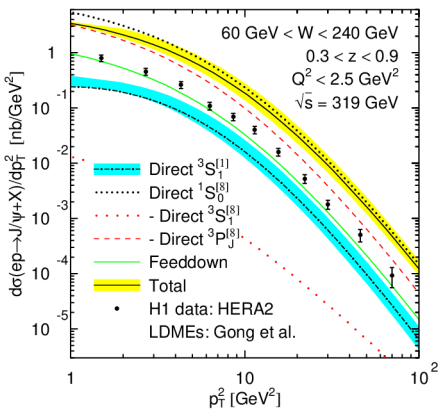

J/ψ Hadroproduction

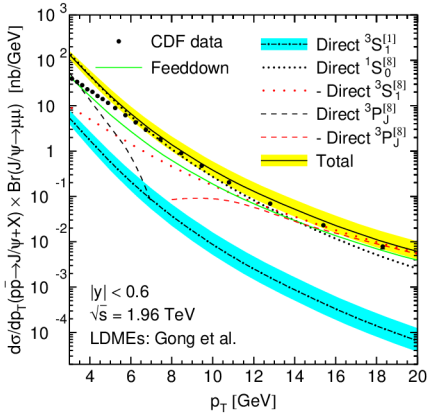

η_c Hadroproduction

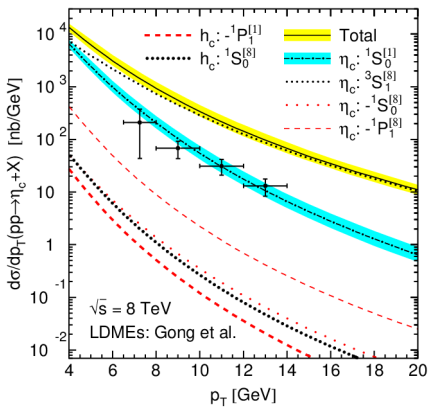

J/ψ + Z Hadroproduction

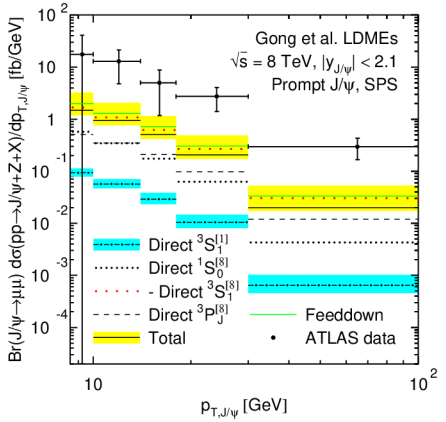

J/ψ Polarization (CDF)

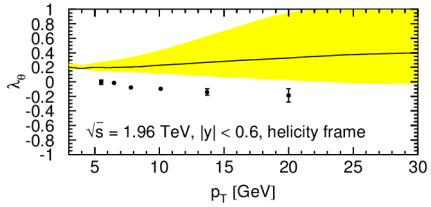

J/ψ Polarization (LHCb)

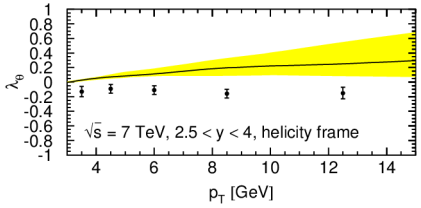

- Fit to J/ψ,ψ(2S), χ_{cJ} hadroprod. yield with $p_T > 7$ GeV.
- $\langle O^{J/\psi}(1S0)\rangle$=0.97 $\pm$0.09, $\langle O^{J/\psi}(3S18)\rangle$=-0.46 $\pm$0.13, $\langle O^{J/\psi}(3P08)\rangle$=-2.14 $\pm$0.56, $\langle O^{\psi(2S)}(1S0)\rangle$=-0.01 $\pm$0.87, $\langle O^{\psi(2S)}(3S18)\rangle$=0.34 $\pm$0.12, $\langle O^{\psi(2S)}(3P08)\rangle$=0.95 $\pm$0.54, $\langle O^{\chi_{c0}}(3S18)\rangle$=0.22 $\pm$0.05 [in 10^{-2} GeV^3 or 10^{-2} GeV^5]
- Ref.: [Gong, Wan, Wang, Zhang, PRL 110, 042002 (2013)]

- Data fitted to is described, other observables not.

3.4 Chao et al. LDMEs

J/ψ Photoproduction

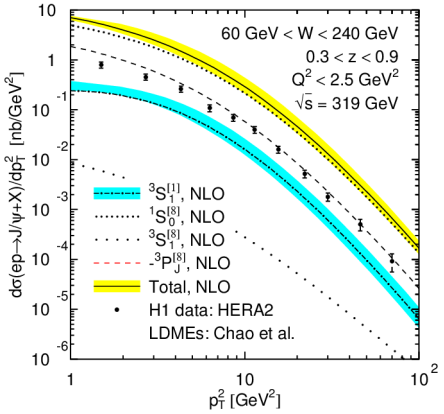

J/ψ Hadroproduction

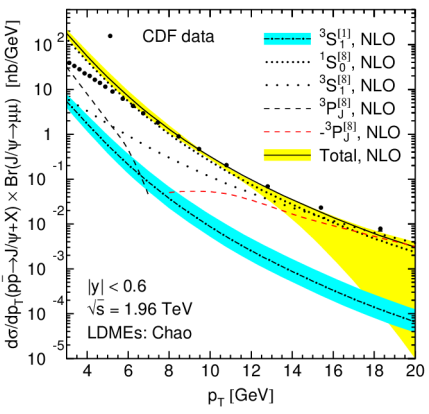

η_c Hadroproduction

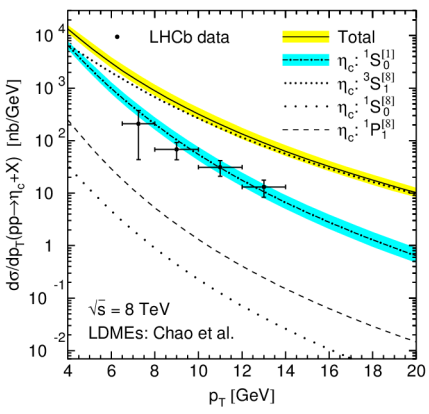

J/ψ + Z Hadroproduction

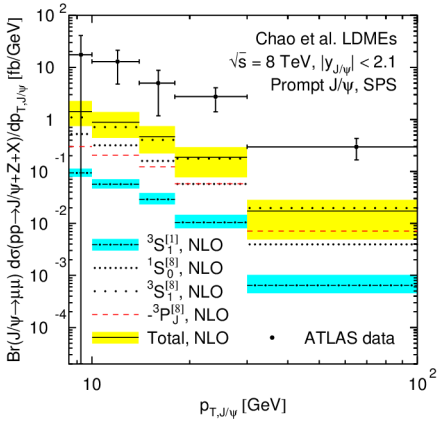

J/ψ Polarization (CDF)

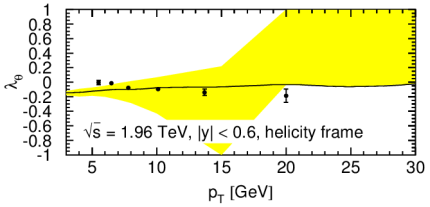

J/ψ Polarization (LHCb)

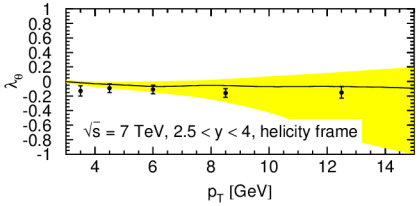

- Fit to CDF J/ψ yield and polarization with $p_T > 7$ GeV.
- $\langle O^{J/\psi}(1S08)\rangle = 8.9 \pm 0.98$, $\langle O^{J/\psi}(3S18)\rangle = 0.30 \pm 0.12$, $\langle O^{J/\psi}(3P08)\rangle = 1.26 \pm 0.47$ [in 10^{-2} GeV^3 or 10^{-2} GeV^5]
- Ref.: [Chao, Ma, Shao, Wang, Zhang, PRL 108, 242004 (2012)]

- Data fitted to is described, other observables not.

3.5 Chao et al. LDMEs: With η_c

J/ψ Photoproduction

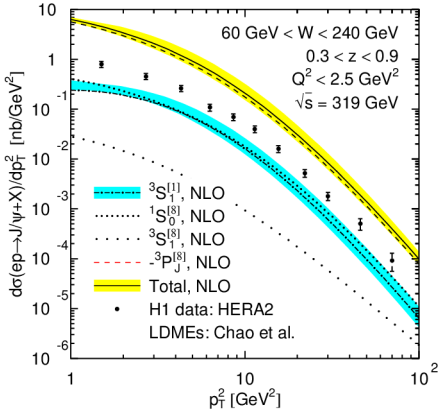

J/ψ Hadroproduction

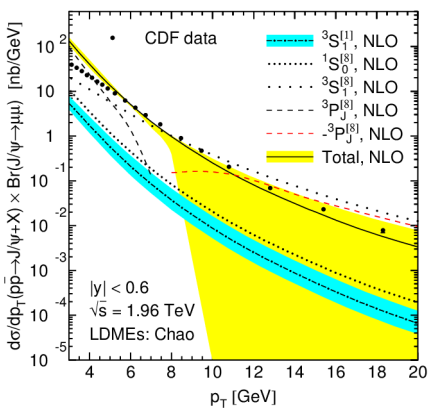

η_c Hadroproduction

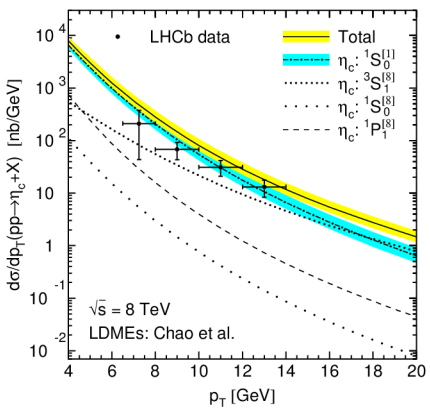

J/ψ + Z Hadroproduction

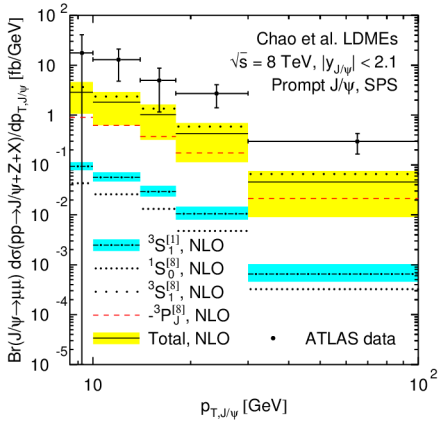

J/ψ Polarization (CDF)

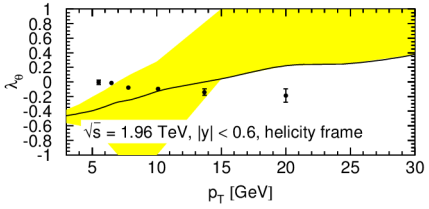

J/ψ Polarization (LHCb)

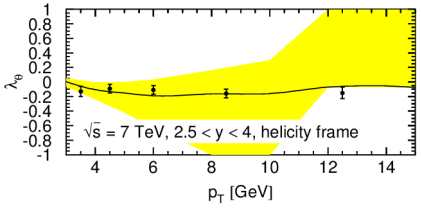

- Fit to CDF J/ψ yield $p_T > 7$ GeV (contraining two linear combinations M_0 and M_1) plus the LHCb η_c production data (constraining $\langle O^{J/\psi}(1S08)\rangle$)
- $\langle O^{J/\psi}(1S08)\rangle = 0.73 \pm 0.73$, $\langle O^{J/\psi}(3S18)\rangle = 1.0 \pm 0.3$, $\langle O^{J/\psi}(3P08)\rangle = 3.8 \pm 1.1$ [in 10^{-2} GeV^3 or 10^{-2} GeV^5]
- Ref.: [Han, Ma, Meng, Shao, Chao, PRL 114 (2015) 092005]

- Nontrivial: Largely unpolarized J/ψ compatible with data (although tensions to CDF data). But: J/ψ hadroproduction $p_T < 7$ GeV, J/ψ photo- and J/$\psi + Z$ production not described.

3.6 Zhang et al. LDMEs

J/ψ Photoproduction

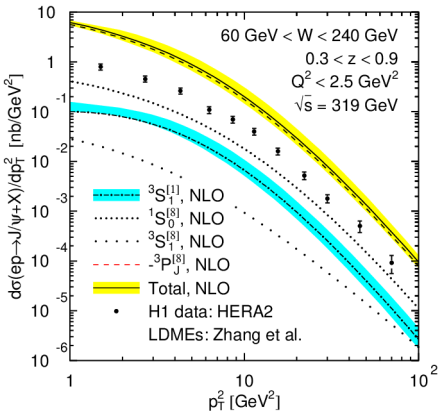

J/ψ Hadroproduction

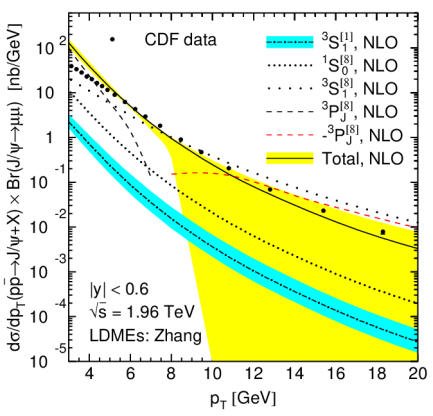

η_c Hadroproduction

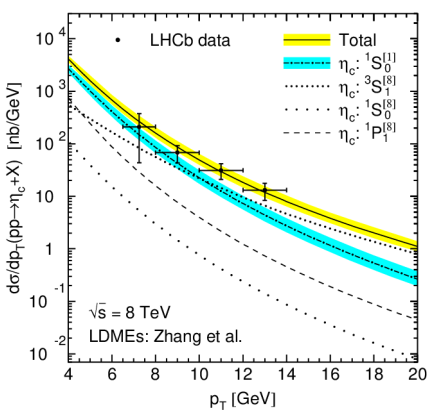

J/ψ + Z Hadroproduction

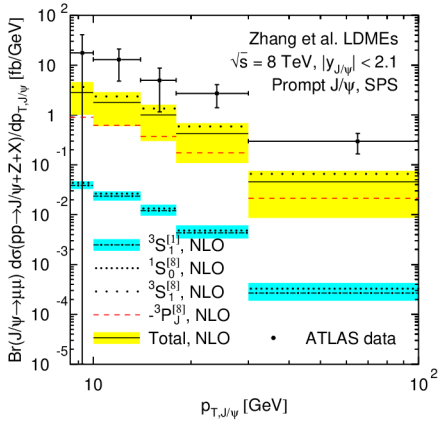

J/ψ Polarization (CDF)

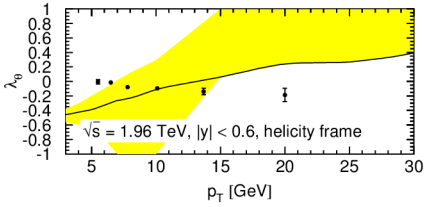

J/ψ Polarization (LHCb)

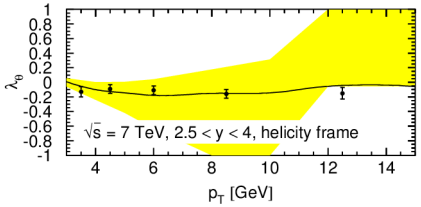

- Fit very similar to Chao et al. fit from previous slide.
- Difference: Also fitted: $\langle O^{J/\psi}(3S11)\rangle=(0.48\pm0.24)\ \mathrm{GeV}^3$
- $\langle O^{J/\psi}(1S08)\rangle=0.74\pm0.30$, $\langle O^{J/\psi}(3S18)\rangle=1.0\pm0.3$, $\langle O^{J/\psi}(3P08)\rangle=3.8\pm0.5$ [in $10^{-2}\ \mathrm{GeV}^3$ or $10^{-2}\ \mathrm{GeV}^5$]
- Ref.: [Zhang, Sun, Sang, Li, PRL 114, (2015) 092006]

- Compared to Chao et al. fit on previous slide: Even better description of η_c production, at the expense of introducing also tensions with other determinations of $\langle O^{J/\psi}(\,^3S_1^{[1]})\rangle$.

3.7 Bodwin et al. LDMEs

J/ψ Photoproduction

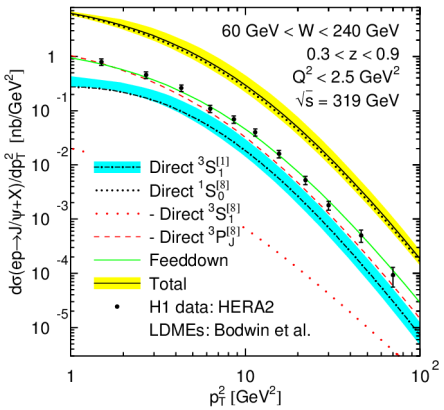

J/ψ Hadroproduction

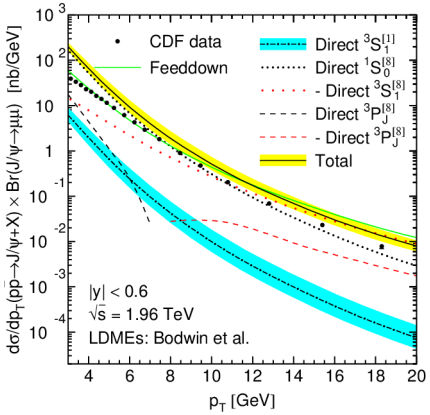

η_c Hadroproduction

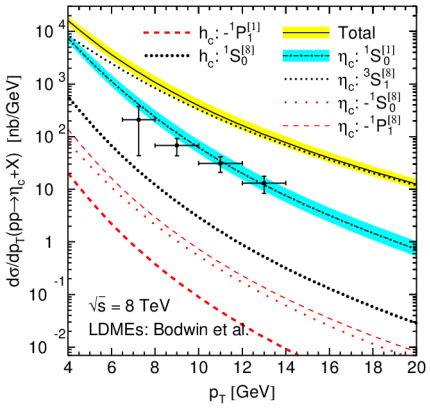

J/ψ + Z Hadroproduction

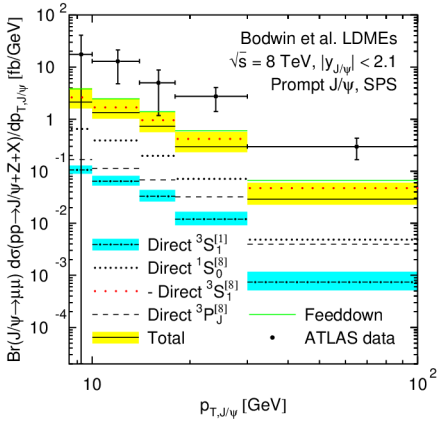

J/ψ Polarization (CDF)

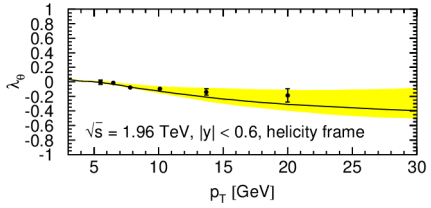

J/ψ Polarization (LHCb)

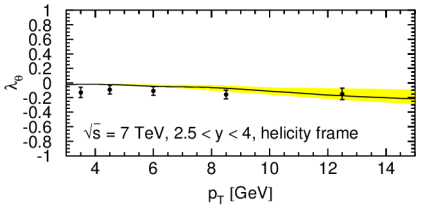

- Fit to J/ψ, ψ(2S), χ_{cJ} hadroproduction yield with $p_T > 3m_H$.
- Includes resummed FFs (we don't here → 2nd plot: small deviations)
- $\langle O^{J/\psi}(1S08)\rangle$=11±1.4, $\langle O^{J/\psi}(3S18)\rangle$=-0.71±0.36, $\langle O^{J/\psi}(3P08)\rangle$=-0.70±0.34, $\langle O^{\psi(2S)}(1S08)\rangle$=3.14±0.79, $\langle O^{\psi(2S)}(3S18)\rangle$=-0.16 ±0.28, $\langle O^{\psi(2S)}(3P08)\rangle$=-0.26±0.27, $\langle O^{\chi_{c0}}(3P01)\rangle$=7.94 ±2.43, $\langle O^{\chi_{c0}}(3S18)\rangle$=0.57±0.13 [$10^{-2}$ GeV$^{3 \text{ or } 5}$]
- Ref.: [Bodwin, Chao, Chung, Kim, Lee, Ma, PRD 93, 034041 (2016)]

- Nontrivial outcome: Unpolarized J/ψ compatible with data.
  But: Small- and mid-p_T J/ψ hadro-; J/ψ photo-, η_c and J/$\psi + Z$ production not described.

Summary

- NRQCD factorization is **candidate theory** for Quarkonium production. Prediction: Universality of LDMEs.
- Ongoing work: Test LDME universality phenomenologically. Most data from J/ψ production and related observables.
- **New results** presented here: Complete NLO NRQCD calculation for **$J/\psi + W$ or Z** production:
  - Cross sections **undershoot ATLAS data** by one order of magnitude. Difference not explicable via double parton scattering.
- These results add to the general picture that there is **no consistent NLO description** of all data with same set of LDMEs yet.
- Some ways forward:
  - Maybe more terms in **v expansion**
  - Maybe higher terms in **α_s expansion**
  - Further resummation of **large logarithms** in various kinematic regions
  - Changes in the formalism (Definition LDMEs in polarized production? Restrict validity to certain kinematic regions and initial/final states? But: Why?)

ADDITIONAL MATERIAL
New $\psi(2S)$ Fit

1001 Data Points of $\psi(2S)$ Hadroproduction Considered

A1

	Collab.	Year	Ref.	Collision	$\sqrt{s}$	(Pseudo-)rapidity	p_T [GeV]	Pol. parameters	Pol. frames
Set 1	CDF	2009	[15]	$p\overline{p}$	1.96 TeV	$\lvert y\rvert < 0.6$	25 bins (2–30)		
Set 2	CDF	1997	[16]	$p\overline{p}$	1.8 TeV	$\lvert \eta\rvert < 0.6$	5 bins (5–20)		
Set 3	CDF	1992	[17]	$p\overline{p}$	1.8 TeV	$\lvert \eta\rvert < 0.5$	4 bins (6–14)		
Set 4	CMS	2012	[18]	pp	7 TeV	3 bins ($\lvert y\rvert < 2.4$)	7–9 bins (5.5–30)		
Set 5	CMS	2015	[19]	pp	7 TeV	4 bins ($\lvert y\rvert < 1.2$)	18 bins (10–75)		
Set 6	CMS	2019	[20]	pp	5.02 TeV	4 bins ($\lvert y\rvert < 0.9$)	2–3 bins (4–30)		
Set 7	LHCb	2012	[21]	pp	7 TeV	$2 < y < 4.5$	11 bins (1–16)	(includes $\psi(2S) \to J/\psi\pi^+\pi^-$)	
Set 8	ATLAS	2014	[22]	pp	7 TeV	3 bins ($\lvert y\rvert < 2$)	10 bins (10–100)	(uses $\psi(2S) \to J/\psi\pi^+\pi^-$)	
Set 9a	ATLAS	2016	[23]	pp	7 TeV	8 bins ($\lvert y\rvert < 2$)	21 bins (8–60)		
Set 9b	ATLAS	2016	[23]	pp	8 TeV	8 bins ($\lvert y\rvert < 2$)	20–24 bins (8–110)		
Set 10	ATLAS	2017	[24]	pp	8 TeV	$\lvert y\rvert < 0.75$	5 bins (10–70)	(uses $\psi(2S) \to J/\psi\pi^+\pi^-$)	
Set 11	ALICE	2017	[25]	pp	13 TeV	$2.5 < y < 4$	11 bins (1–16)		
Set 12	ALICE	2014	[25]	pp	7 TeV	$2.5 < y < 4$	8 bins (1–12)		
Set 13	ALICE	2016	[27]	pp	8 TeV	$2.5 < y < 4$	8 bins (1–12)		
Set 14	CMS	2018	[28]	pp	13 TeV	4 bins ($\lvert y\rvert < 1.2$)	9 bins (20–100)		
Set 15a	LHCb	2020	[29]	pp	7 TeV	5 bins ($2.0 < y < 4.5$)	11 bins (3.5–14)		
Set 15b	LHCb	2020	[29]	pp	13 TeV	5 bins ($2.0 < y < 4.5$)	14–17 bins (2–20)		
Set 16	ATLAS	2018	[30]	pp	5.02 TeV	3 bins ($\lvert y\rvert < 2$)	5 bins (8–40)		
Set P1	LHCb	2014	[31]	pp	7 TeV	5 bins ($2 < y < 4.5$)	5 bins (3.5–15)	λ_θ, λ_ϕ, $\lambda_{\theta\phi}$	HX, CS
Set P2	CDF	2007	[32]	$p\overline{p}$	1.96 TeV	$\lvert y\rvert < 0.6$	3 bins (5–30)	λ_θ	HX
Set P3	CDF	2000	[33]	$p\overline{p}$	1.8 TeV	$\lvert y\rvert < 0.6$	3 bins (5.5–20)	λ_θ	HX
Set P4	CMS	2013	[34]	pp	7 TeV	3 bins ($\lvert y\rvert < 1.5$)	4 bins (14–50)	λ_θ, λ_ϕ, $\lambda_{\theta\phi}$	HX, CS, PX

Results of Four Different Fits

A2

	Fit A	Fit B	Fit C	Fit D
Data fitted to	All data	All unpolarized data	All data with $p_T > 7$ GeV	All unpolarized data with $p_T > 7$ GeV
Number of data points	1001	737	816	644
$O_1 = \langle \mathcal{O}^{\psi(2S)}({}^1S_0^{[8]}) \rangle / \mathrm{GeV}^3$	0.000958 ± 0.000129	0.0100 ± 0.0003	0.00835 ± 0.00096	0.0119 ± 0.0020
$O_2 = \langle \mathcal{O}^{\psi(2S)}({}^3S_1^{[8]}) \rangle / \mathrm{GeV}^3$	0.00149 ± 0.00001	0.000537 ± 0.000029	0.00276 ± 0.00012	0.00225 ± 0.00025
$O_3 = \langle \mathcal{O}^{\psi(2S)}({}^3P_0^{[8]}) \rangle / \mathrm{GeV}^5$	-0.000583 ± 0.000056	-0.00489 ± 0.00012	0.00865 ± 0.00055	0.00612 ± 0.00119
χ^2/d.o.f.	14.3	12.7	2.7	2.5
Cov. matrix eigenvector $\mathbf{v_1}$	$(0.917, -0.096, -0.387)$	$(0.906, -0.096, -0.413)$	$(0.867, -0.104, -0.487)$	$(0.855, -0.107, -0.508)$
Cov. matrix eigenvector $\mathbf{v_2}$	$(0.394, 0.072, 0.916)$	$(0.419, 0.061, 0.906)$	$(0.497, 0.125, 0.859)$	$(0.518, 0.121, 0.846)$
Cov. matrix eigenvector $\mathbf{v_3}$	$(0.060, 0.993, -0.103)$	$(0.062, 0.993, -0.096)$	$(0.029, 0.987, -0.160)$	$(0.029, 0.987, -0.159)$
$V_1 = \mathbf{v_1} \cdot (O_1, O_2, O_3)$	0.000962 ± 0.000141	0.01103 ± 0.00030	0.00275 ± 0.00110	0.00680 ± 0.00234
$V_2 = \mathbf{v_2} \cdot (O_1, O_2, O_3)$	-0.000050 ± 0.000013	-0.000200 ± 0.000014	0.01192 ± 0.00013	0.01161 ± 0.00014
$V_3 = \mathbf{v_3} \cdot (O_1, O_2, O_3)$	0.001597 ± 0.000006	0.001619 ± 0.000006	0.001577 ± 0.000006	0.001593 ± 0.000006
Rel. errors of $\{V_1, V_2, V_3\}$	$\{14.7\%, 26.8\%, 0.4\%\}$	$\{2.7\%, 7.2\%, 0.4\%\}$	$\{40.1\%, 1.1\%, 0.4\%\}$	$\{34.4\%, 1.2\%, 0.4\%\}$

- In fit C and D, V_2 and V_3 correspond to Chao et al.'s $\frac{M_0}{\mathrm{GeV}^3} = 0.02 \pm 0.06$ and $\frac{M_1}{\mathrm{GeV}^3} = 0.0012 \pm 0.006$, $\boldsymbol{v}_2$ and $\boldsymbol{v}_3$ to their corresponding vectors $\boldsymbol{M}_0 = (0.5, 0, 0.87)$ and $\boldsymbol{M}_1 = (0, 0.97, -0.24)$.

Main Features in Example Plots

A3

Fit A (all data)	**Fit B** (all unpolarized data)	**Fit C** (all data $p_T > 7$ GeV)	**Fit D** (all unpolarized data $p_T > 7$ GeV)

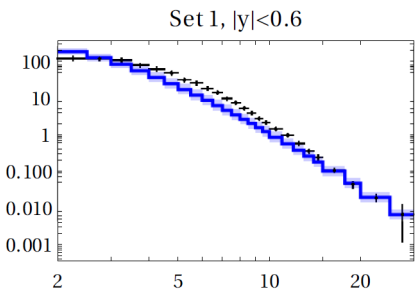

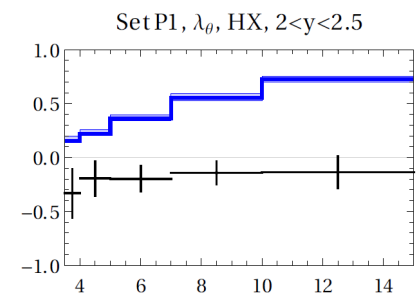

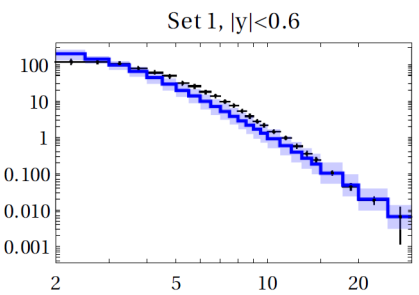

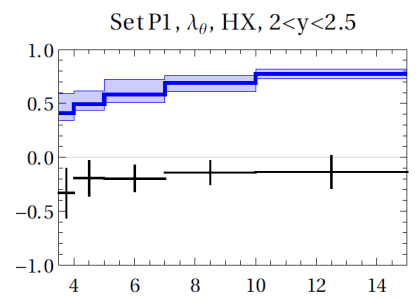

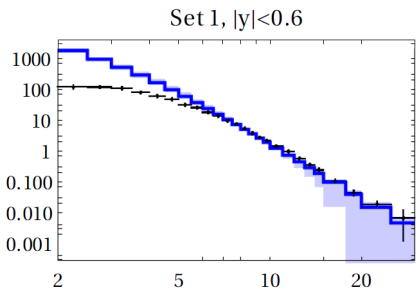

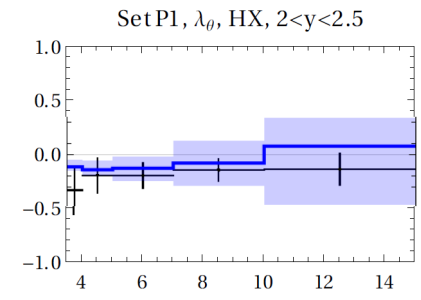

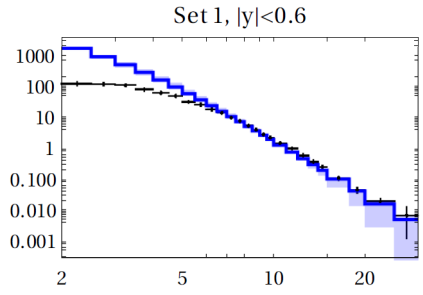

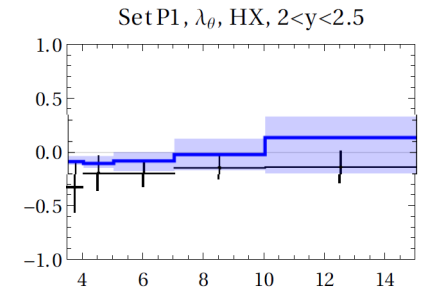

Details Fit A (All Data)

A4

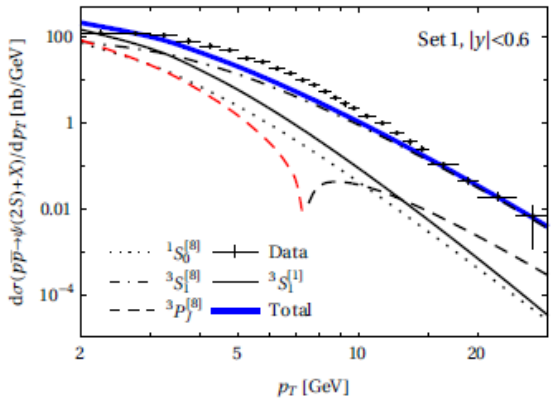

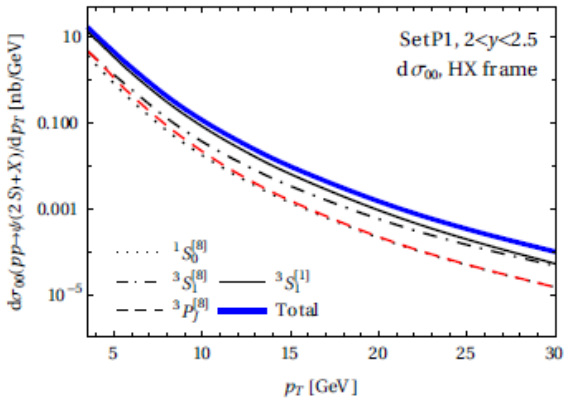

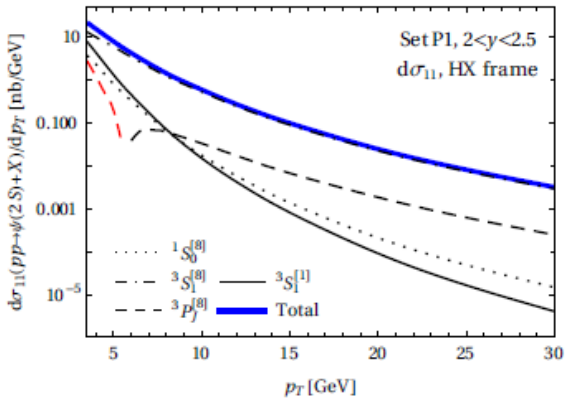

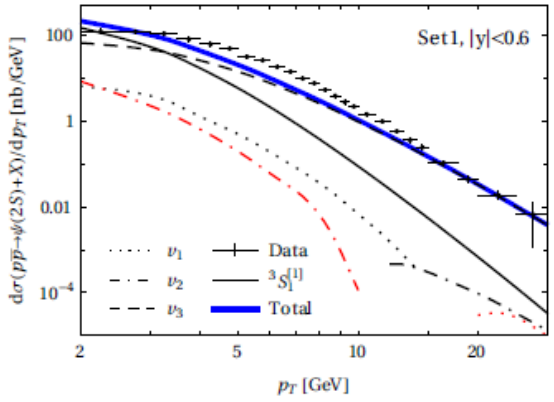

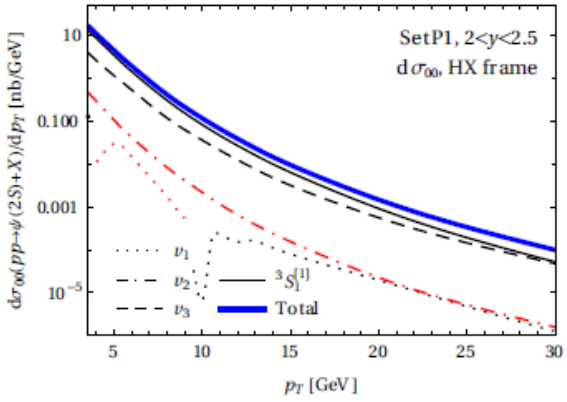

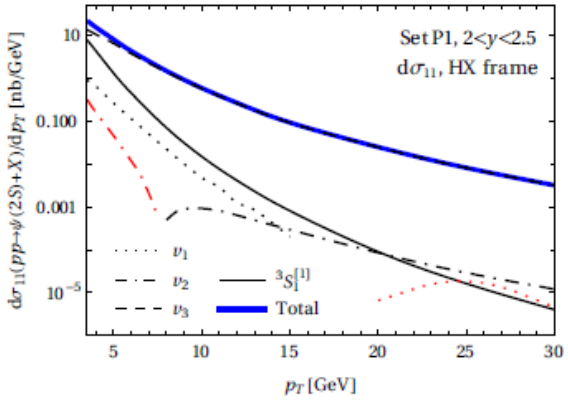

Details Fit B (All Unpolarized Data)

A5

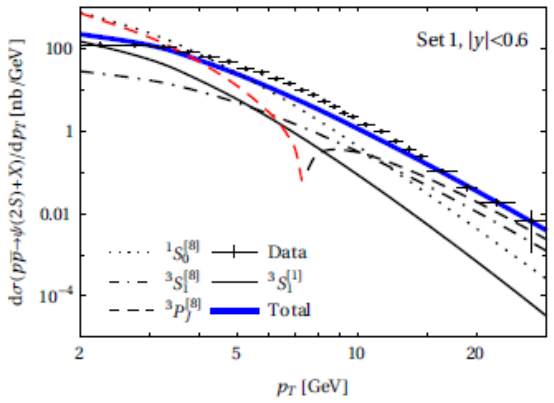

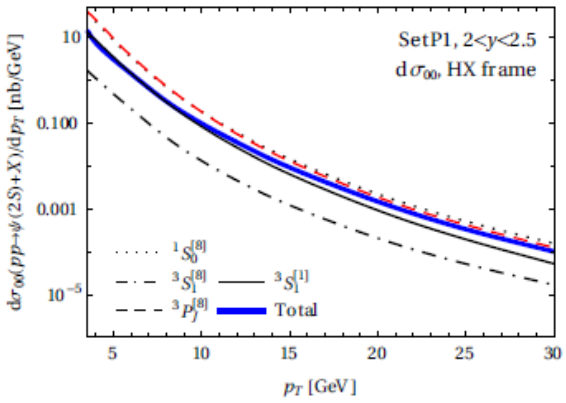

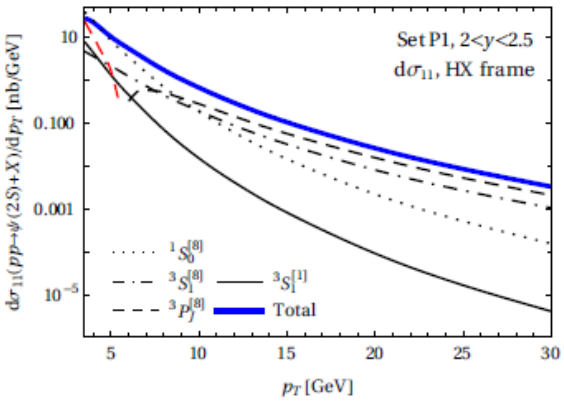

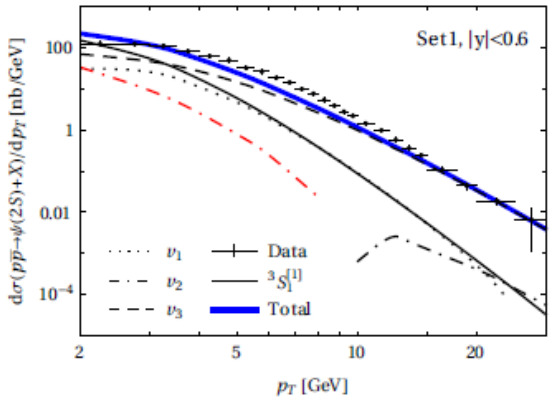

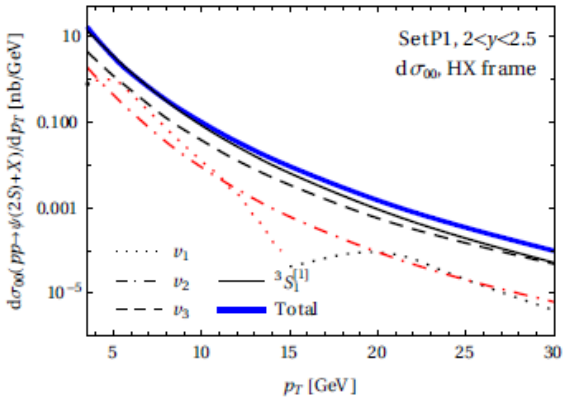

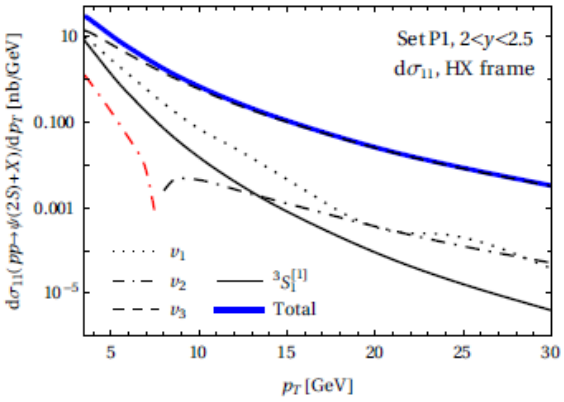

Details Fit C (All Data $p_T > 7$ GeV)

A6

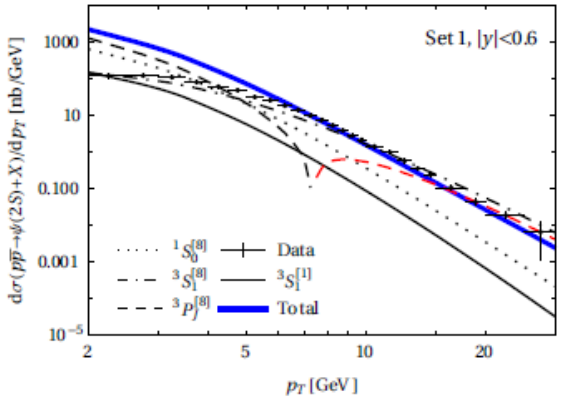

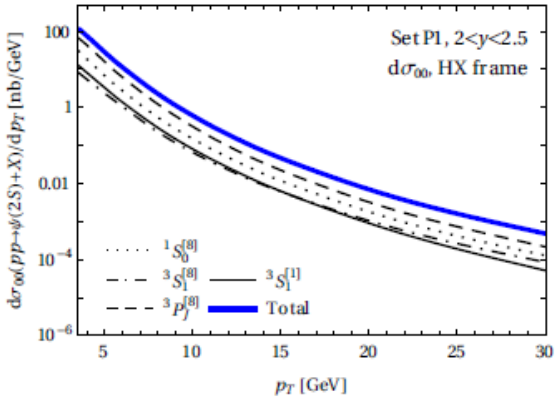

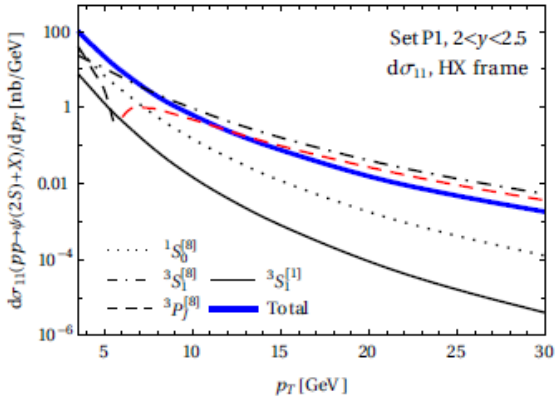

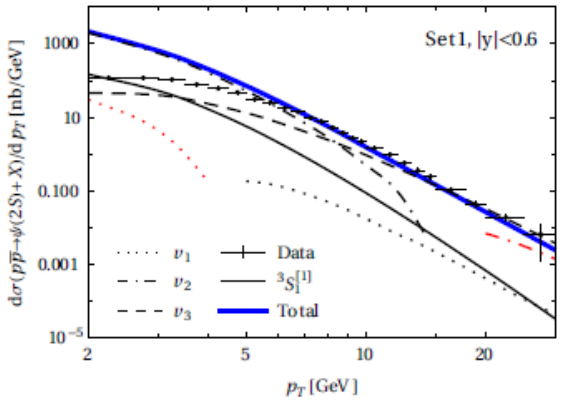

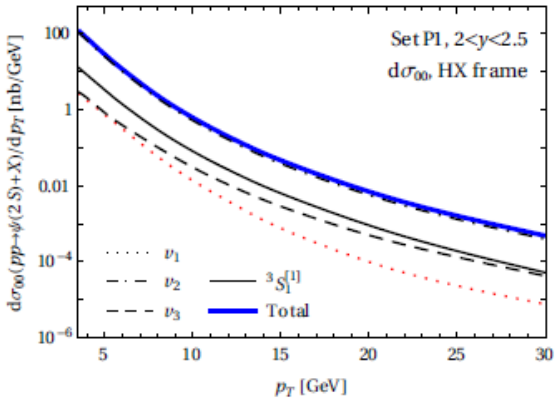

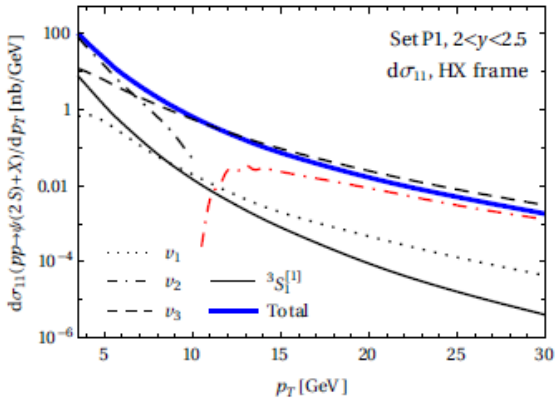

Details Fit D (All Unpolarized Data $p_T > 7$ GeV)

A7

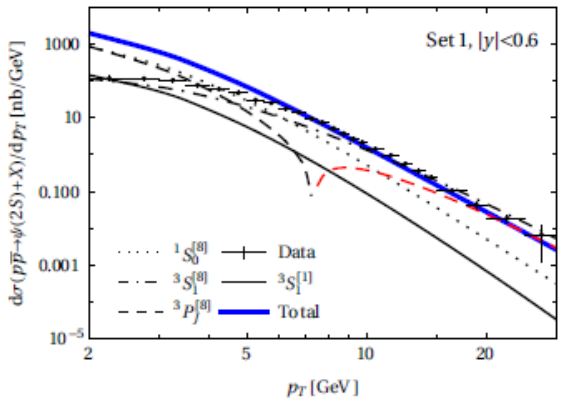

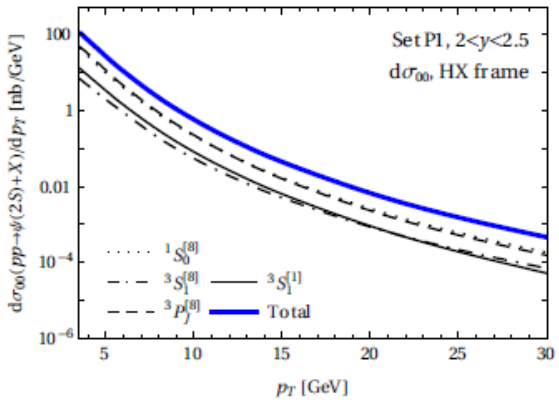

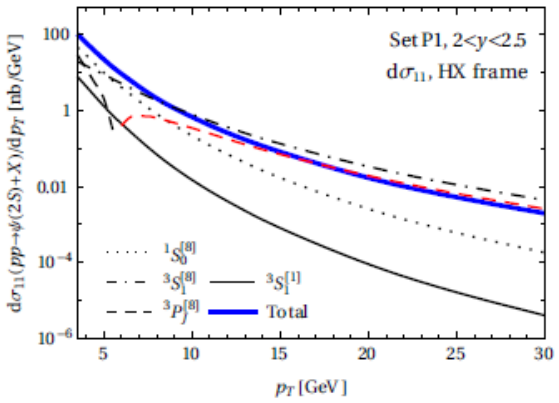

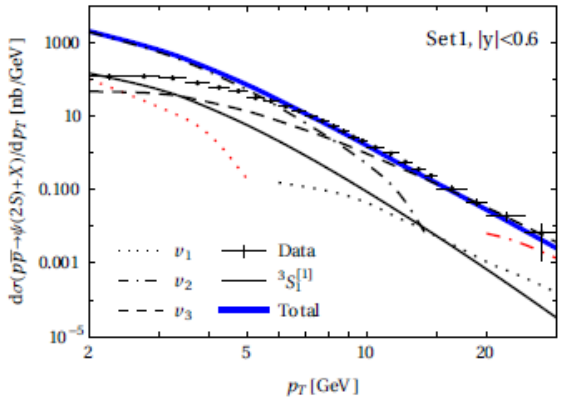

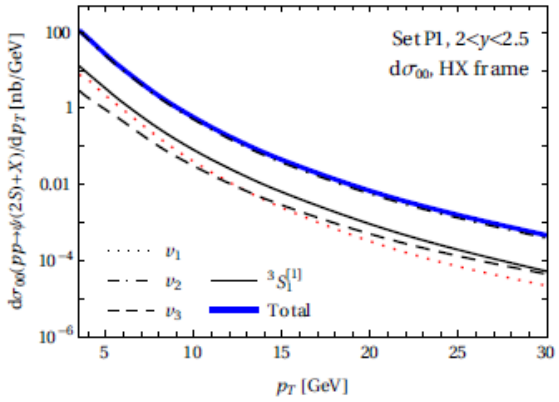

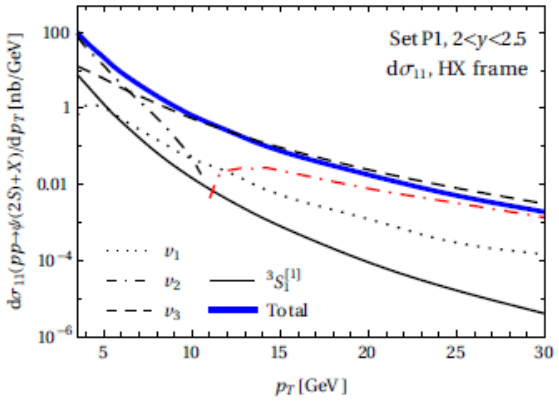

BACKUP MATERIAL

Difficulties Starting at NLO

B1

- Virtual Corrections:

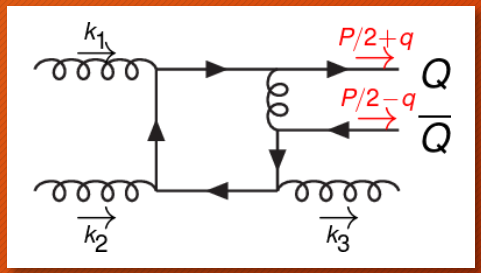

- $q \longrightarrow 0$: **Linear dependent** propagator momenta
- Derivatives w.r.t. q in P states: **Double** propagator momenta

- Real Corrections:

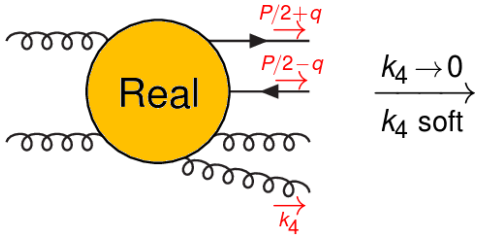

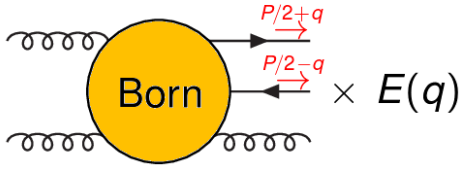

$$A_{\text{soft}}(q) = A_{Born}(q) \cdot E(q)$$

$$A_{\text{soft,p}} = A'_{\text{soft}}(0) = A_{\text{Born,p}} E(0) + A_{\text{Born,s}} E'(0)$$

- New types of soft singularites due to **derivatives of eikonal factor** in P states
- These cancel against **NLO corrections to S wave LDMEs** (calculable within NRQCD)

⟹ Mixing of different Fock state contributions

Sensitivity to PDF Set Choice

B2

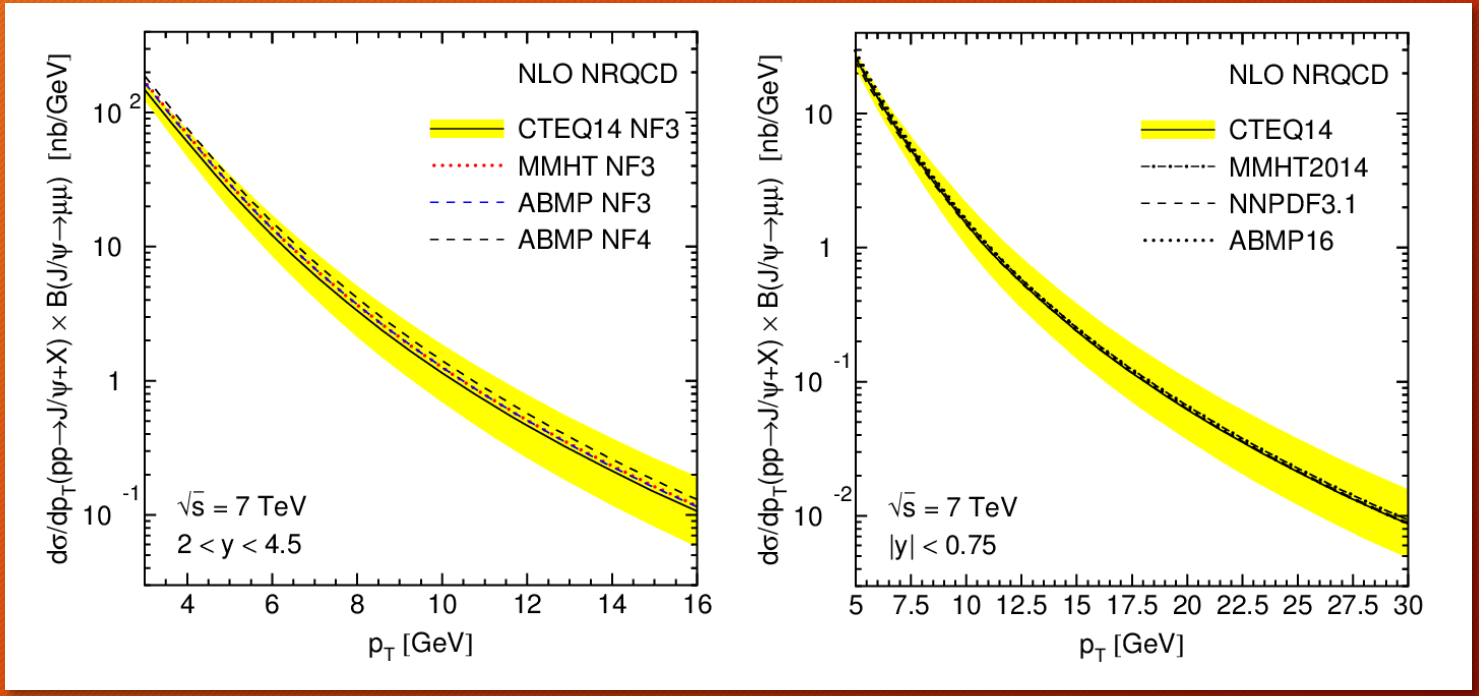

- Yellow bands: Scale variations

Details Butenschön et al. Fit

B3

- Hadro- and photoproduction within scale uncertainties well described:

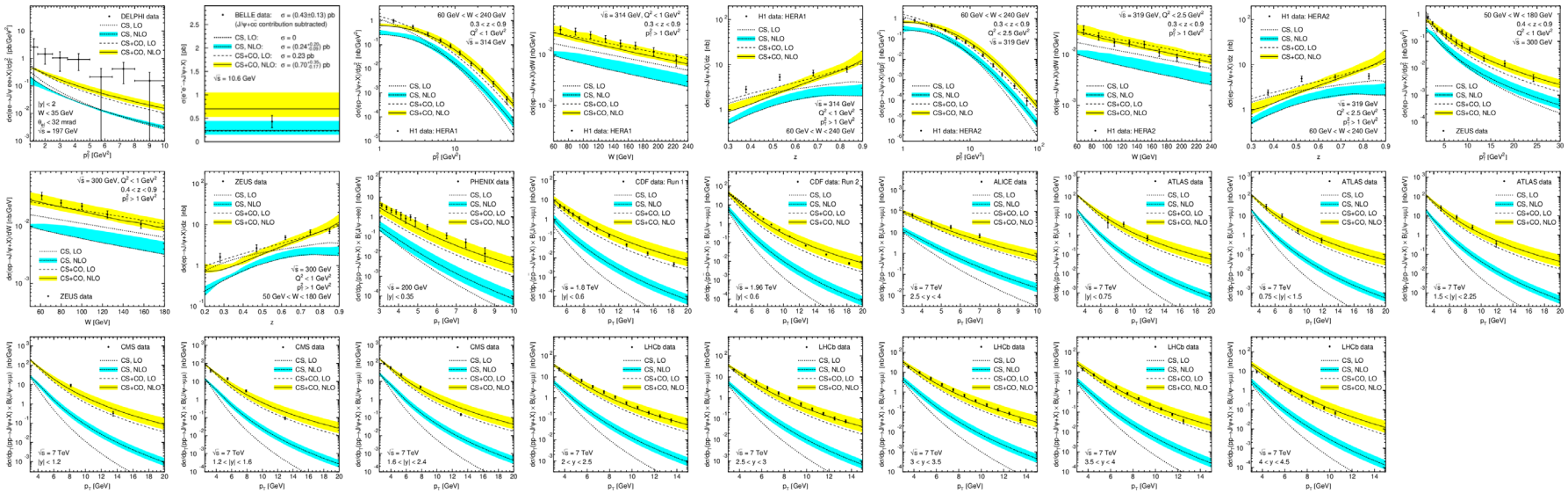

$$\langle O^{J/\psi}[^1S_0^{[8]}]\rangle = (4.97 \pm 0.44) \times 10^{-2}\ \text{GeV}^3 \qquad \langle O^{J/\psi}[^3S_1^{[8]}]\rangle = (2.24 \pm 0.59) \times 10^{-3}\ \text{GeV}^3$$

$$\langle O^{J/\psi}[^3P_0^{[8]}]\rangle = (-1.61 \pm 0.20) \times 10^{-2}\ \text{GeV}^5$$

[MB, Kniehl: PRL 104 (2010) 072001, PRL 106 (2011) 022003, PRD 84 (2011) 051501]

Details Butenschön et al. Fit

B3

- Hadro- and photoproduction within scale uncertainties well described:

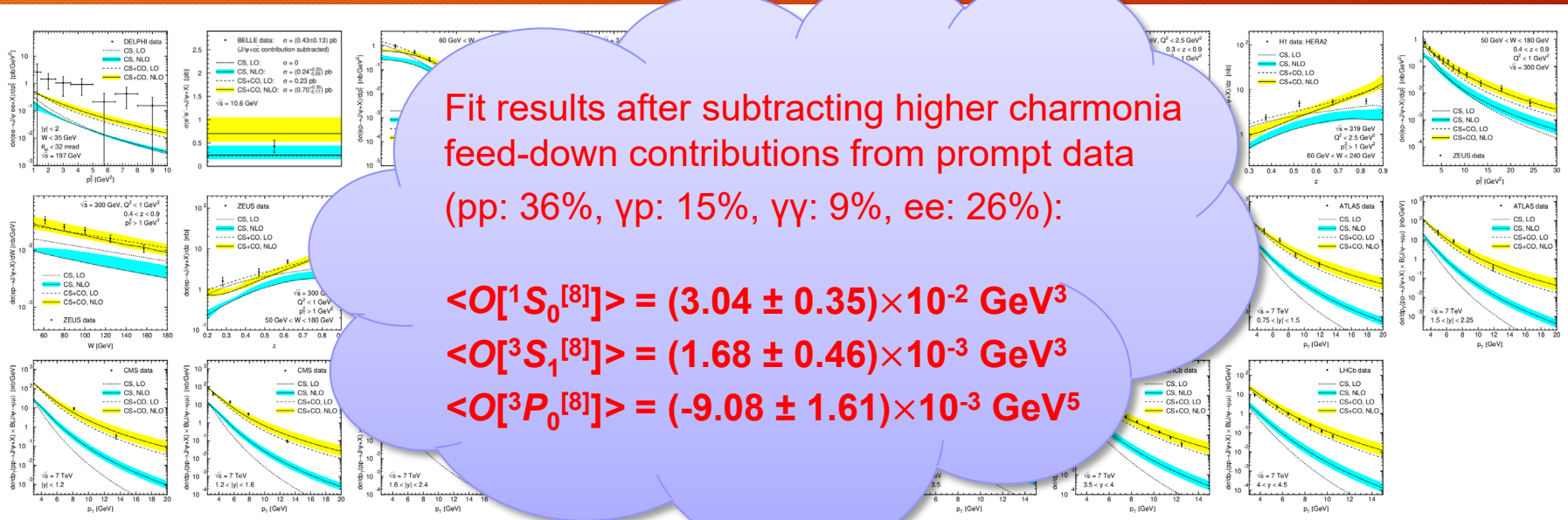

Fit results after subtracting higher charmonia feed-down contributions from prompt data (pp: 36%, γp: 15%, γγ: 9%, ee: 26%):

$\langle O[^1S_0^{[8]}] \rangle = (3.04 \pm 0.35) \times 10^{-2}\ \text{GeV}^3$

$\langle O[^3S_1^{[8]}] \rangle = (1.68 \pm 0.46) \times 10^{-3}\ \text{GeV}^3$

$\langle O[^3P_0^{[8]}] \rangle = (-9.08 \pm 1.61) \times 10^{-3}\ \text{GeV}^5$

$$\langle O^{J/\psi}[^1S_0^{[8]}] \rangle = (4.97 \pm 0.44) \times 10^{-2}\ \text{GeV}^3 \qquad \langle O^{J/\psi}[^3S_1^{[8]}] \rangle = (2.24 \pm 0.59) \times 10^{-3}\ \text{GeV}^3$$

$$\langle O^{J/\psi}[^3P_0^{[8]}] \rangle = (-1.61 \pm 0.20) \times 10^{-2}\ \text{GeV}^5$$

[MB, Kniehl: PRL 104 (2010) 072001, PRL 106 (2011) 022003, PRD 84 (2011) 051501]

Details Butenschön et al. Fit

- Hadro- and photoproduction within scale uncertainties well described:

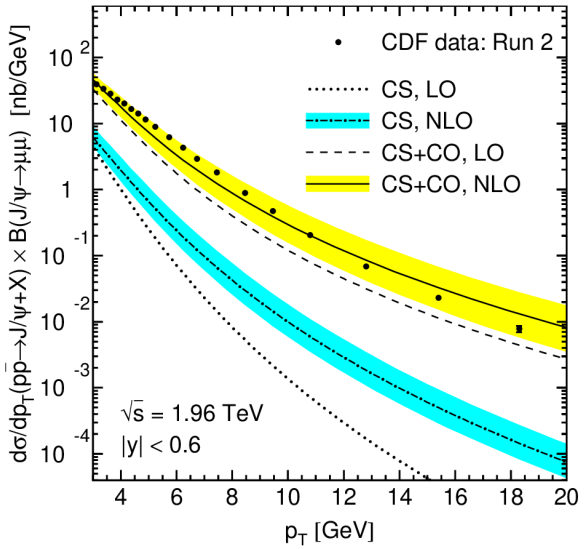

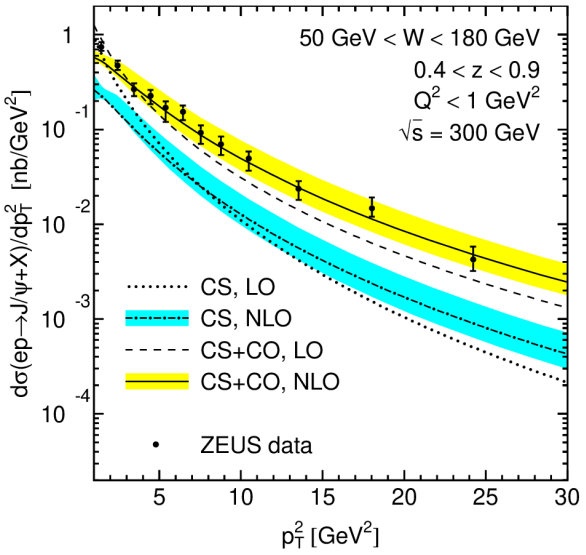

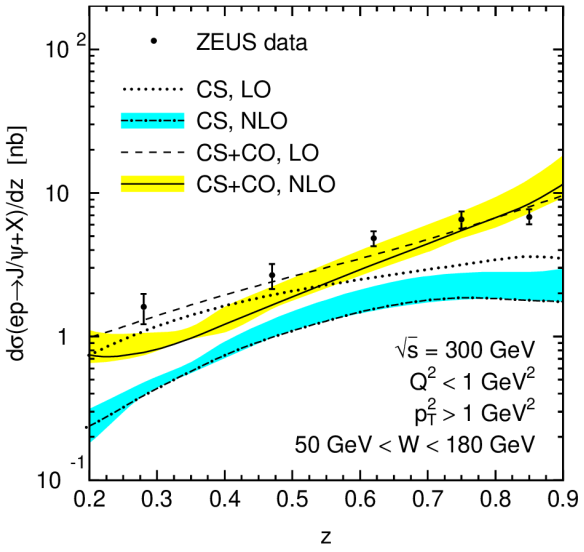

$$\langle O^{J/\psi}[^1S_0^{[8]}]\rangle = (4.97 \pm 0.44) \times 10^{-2}\ \text{GeV}^3 \qquad \langle O^{J/\psi}[^3S_1^{[8]}]\rangle = (2.24 \pm 0.59) \times 10^{-3}\ \text{GeV}^3$$

$$\langle O^{J/\psi}[^3P_0^{[8]}]\rangle = (-1.61 \pm 0.20) \times 10^{-2}\ \text{GeV}^5$$

[MB, Kniehl: PRL 104 (2010) 072001, PRL 106 (2011) 022003, PRD 84 (2011) 051501]

Details Butenschön et al. Fit

B3

- Hadro- and photoproduction within scale uncertainties well described:

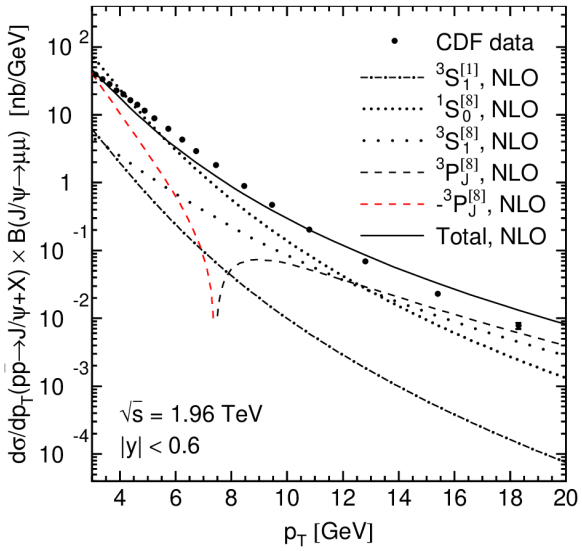

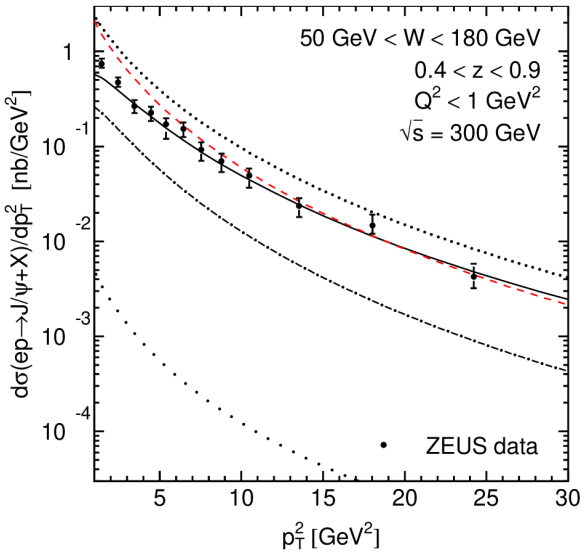

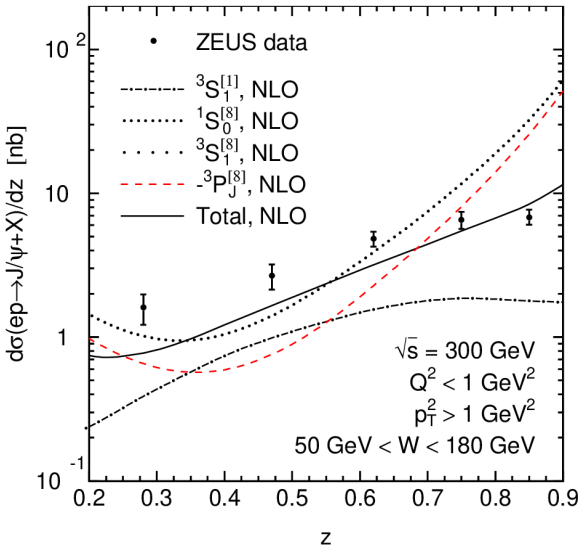

$$\langle O^{J/\psi}[^1S_0^{[8]}]\rangle = (4.97 \pm 0.44) \times 10^{-2}\ \text{GeV}^3 \qquad \langle O^{J/\psi}[^3S_1^{[8]}]\rangle = (2.24 \pm 0.59) \times 10^{-3}\ \text{GeV}^3$$

$$\langle O^{J/\psi}[^3P_0^{[8]}]\rangle = (-1.61 \pm 0.20) \times 10^{-2}\ \text{GeV}^5$$

[MB, Kniehl: PRL 104 (2010) 072001, PRL 106 (2011) 022003, PRD 84 (2011) 051501]

Details Chao et al. Fit With η_c

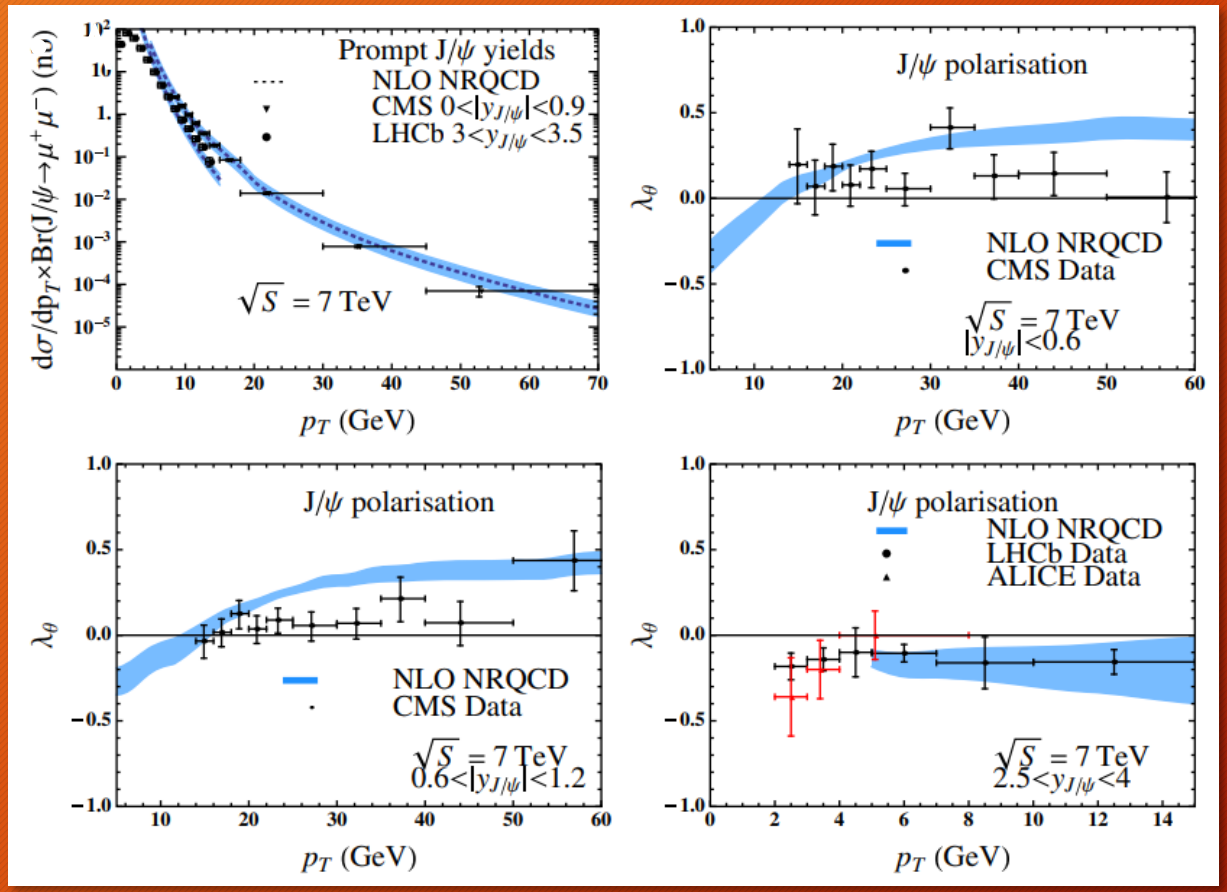

Plots taken from

[Han, Ma, Meng, Shao, Chao: PRL 114 (2015) 092005]

Details Zhang et al. Fit

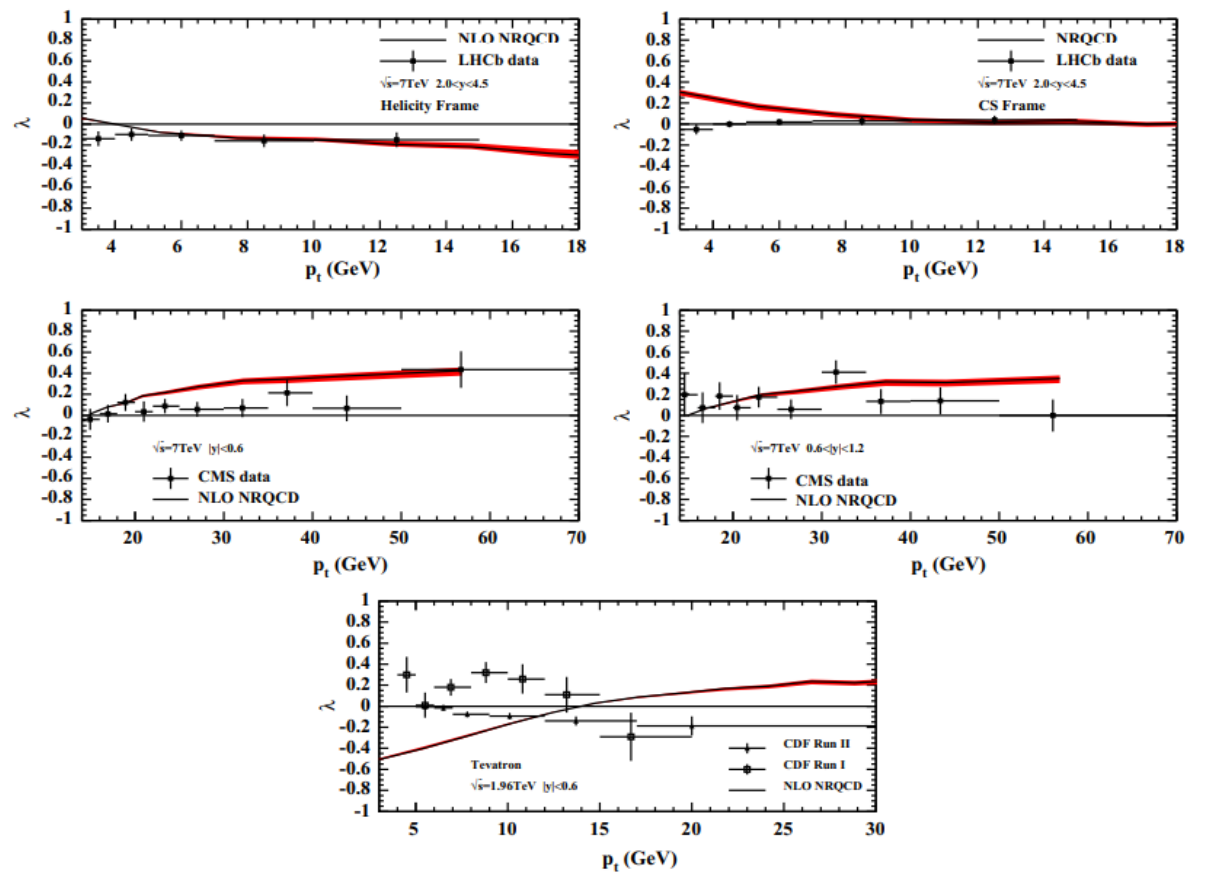

Plots taken from

[Zhang, Sun, Sang, Li: PRL 114 (2015) 092006]

J/ψ Polarization

- **Angular distribution** of decay lepton l^+ in J/ψ rest frame
  ➡ Polarization observables λ, μ, ν:

$$\frac{d\Gamma(J/\psi \to l^+ l^-)}{d\cos\theta\, d\phi} \propto 1 + \lambda\cos^2\theta + \mu\sin(2\theta)\cos\phi + \frac{\nu}{2}\sin^2\theta\cos(2\phi)$$

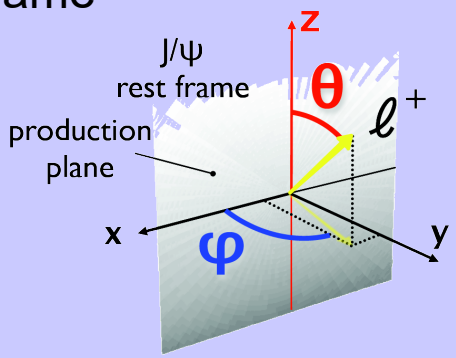

- Depends on choice of **coordinate system:**
  - Helicity frame: z axis $\| -(\vec{p}_\gamma + \vec{p}_p)$
  - Collins-Soper frame: z axis $\| \vec{p}_\gamma/|\vec{p}_\gamma| - \vec{p}_p/|\vec{p}_p|$
  - Target frame: z axis $\| -\vec{p}_p$

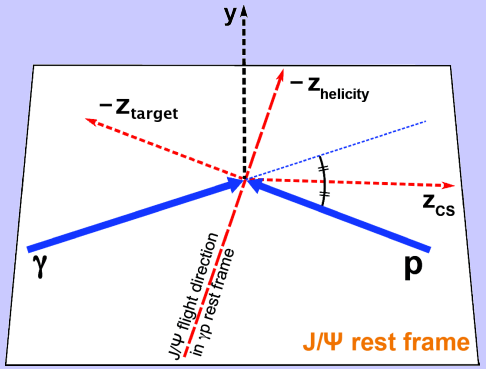

- **In Calculation:** Plug in explicit expressions for $c\bar{c}[n]$ spin polarization vectors according to

$$\lambda = \frac{d\sigma_{11} - d\sigma_{00}}{d\sigma_{11} + d\sigma_{00}}, \quad \mu = \frac{\sqrt{2}\,\mathrm{Re}\, d\sigma_{10}}{d\sigma_{11} + d\sigma_{00}}, \quad \nu = \frac{2d\sigma_{1,-1}}{d\sigma_{11} + d\sigma_{00}}$$

- We use the CO LDME set with feed-down contributions subtracted.

J/ψ Polarization in Photoproduction: p_T Distribution

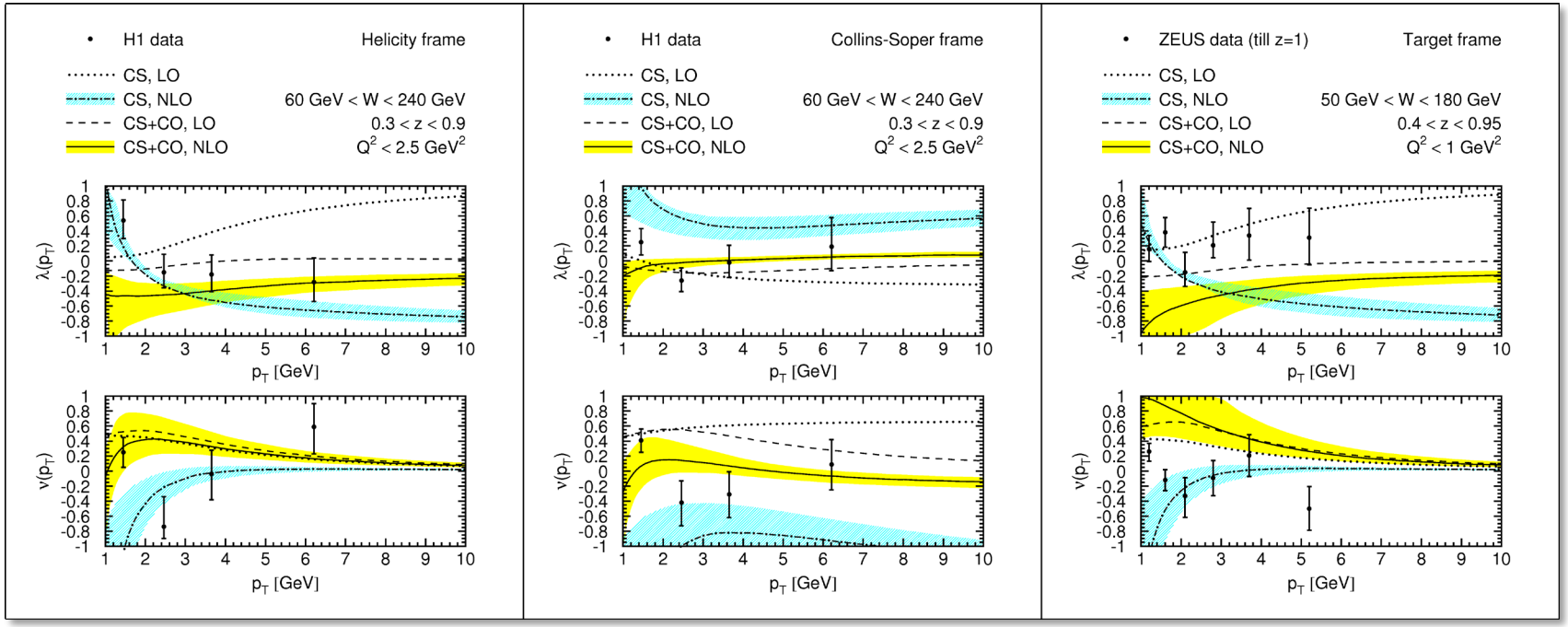

[MB, Kniehl: PRL 107, 232001]

- Bands: Uncertainties due to scale variation and CO LDMEs.
- **CSM** predicts **longitudinal** *J/ψ* at high p_T.
- **CS+CO:** largely **unpolarized** *J/ψ* at high p_T. α_s expansion converges better.
- H1 and ZEUS **data not precise** enough to discriminate CSM / NRQCD.

J/ψ Polarization in Photoproduction: z Distribution

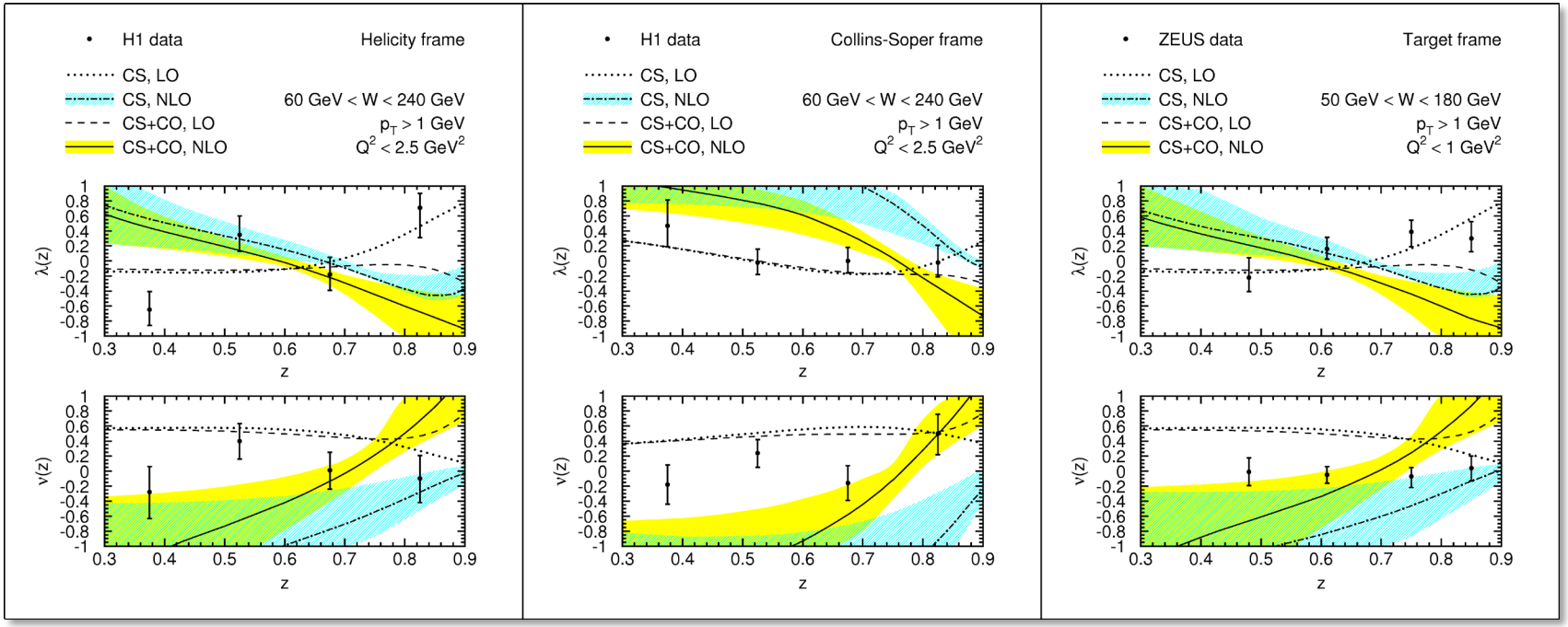

[MB, Kniehl: PRL 107, 232001]

- Bands: Uncertainties due to scale variation and CO LDMEs.
- **Scale** uncertainties very large.
- **Error bands** of CSM and NRQCD largely **overlap**.

➡ p_T distribution better suited to discriminate production mechanisms than z.

J/ψ Polarization in Hadroproduction

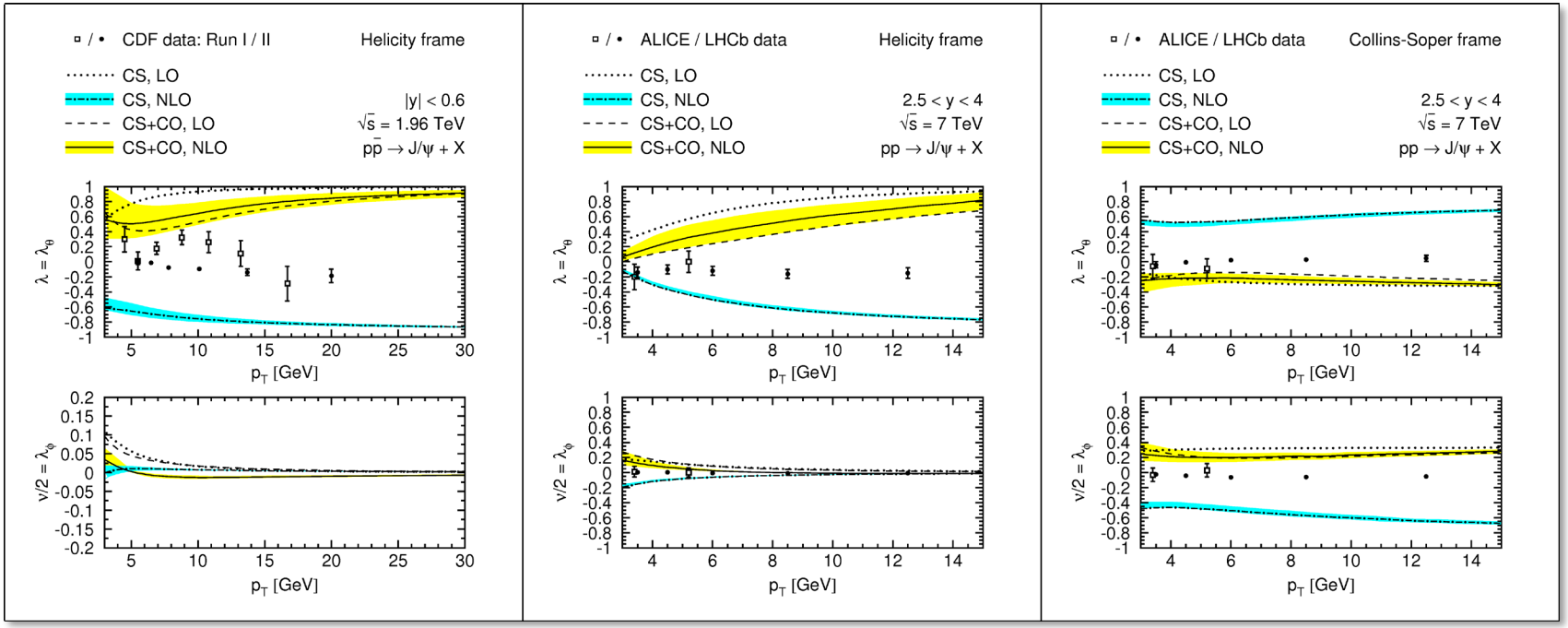

[MB, Kniehl: PRL 108, 172002]

- **Helicity frame**: NRQCD predicts strong **transverse** polarization at high p_T.
- **Collins-Soper frame**: NRQCD predicts slightly longitudinal J/ψ.
- **Disagreement** with CDF Run II data, and with new ALICE and LHCb data.
  ➡ **Challenge to LDME universality!**